村松慎一	パーキンソン病モデルサルへのES細胞由来神経幹細胞の移植	日本再生医療学会雑誌	3	39-44	2004
村松慎一	遺伝子治療. 特集 パーキンソン病	日本臨床	62(9):	1648-1652	2004
星美奈子	新規毒性物質「アミロスフェロイド」の形成と神経細胞死	生化学　総説	76	631-639	2004
星美奈子	新規球状毒性会合体「アミロスフェロイド」の同定-アルツハイマー病発症に置ける神経細胞死機構の解明に向けて	Dementia Japan	18	19-28	2004
星美奈子	βアミロイド自己組織化による神経毒性の発現-新規毒性物質「アミロスフェロイド」とアルツハイマー病	化学と工業	第57巻、第5号	519-521	2004
星美奈子	神経変性疾患研究の最前線　特集号監修:特集にあたって	Bioindustry	21	5-7	2004
星美奈子	アミロスフェロイド-タンパク質の自己組織化と神経変性疾患	Bioindustry	21	67-74	2004
星美奈子	球状βアミロイド凝集体アミロスフェロイドー蛋白質の自己組織化と神経細胞死	Cognition and Dementia	3	359-366	2004

III. 研究成果の刊行物・別刷り

低温生物工学会誌〔Cryobiology and Cryotechnology〕, Vol. 51, No. 2, 137～140, 2005

β-アミロイド凝集に及ぼすトレハロースの効果

[1]東京工業大学バイオ研究基盤支援総合センター, [2]東京工業大学フロンティア創造共同研究センター
[3]東京工業大学大学院生命理工学研究科, [4]三菱化学生命科学研究所アルツハイマー病研究グループ
渡邉亜沙子[1], 岡畑 恵雄[2,3], 古澤 宏幸[3], 星 美奈子[3,4], 櫻井 実[1]

The Effect of Trehalose on the Aggregation of β-amyloid

Asako WATANABE[1], Yoshio OKAHATA[2,3], Hiroyuki FURUSAWA[3], Minako HOSHI[3,4] and Minoru SAKURAI[1]

[1]*Center for Biological Resources and Informatics, Tokyo Institute of Technology, 4259 Nagatsuta-cho, Midori-ku, Yokohama 226-8501, Japan*

[2]*Frontier Collaborative Research Center, Tokyo Institute of Technology, 4259 Nagatsuta-cho, Midori-ku, Yokohama 226-8501, Japan*

[3]*Department of Biomolecular Engineering, Tokyo Institute of Technology, 4259 Nagatsuta-cho, Midori-ku, Yokohama 226-8501, Japan*

[4]*Research Group for Alzheimer's Disease, Mitsubishi Kagaku Institute of Life Sciences, 11 Minamiooya, Machida, Tokyo 194-8511, Japan*

The effect of trehalose on the aggregation of β-amyloid (Aβ) was investigated using quartz crystal microbalance (QCM) and circular dichroism spectroscopy (CD). Here we prepared three types of host Aβ-guest Aβ systems differing in a combination of their secondary structures: namely, β-sheet-β-sheet (system ①), β-sheet-random coil (system②) and random coil-random coil (system③). The host Aβ was fixed on the electrode of QCM, and the guest Aβ was dissolved in a buffer solution. The host-guest interaction was monitored through a frequency shift (ΔF) of the quartz vibration: a larger ΔF value means the occurrence of a larger degree of host-guest aggregation. When disaccharide (trehalose, neotrehalose or maltose) was added in the above system, the time dependent profile of ΔF was significantly affected. In systems ① and ②, any of these disaccharides depressed significantly the host-guest aggregation: maltose and trehalose exhibited the strongest effect in systems ① and ②, respectively. Interestingly, in system③, trehalose rather promoted the aggregation compared with the control (without disaccharide), while both maltose and neotrehalose depressed the aggregation as much as in the cases of systems ① and ②. The results of systems ② and ③ imply that trehalose more strongly interacts with Aβ in a random coil than that in β-sheets. In fact, CD measurements indicated that trehalose retarded the transformation of Aβ from a random coil to β-sheet. Taken together, these results open up the possibility that trehalose modifies the aggregation process of Aβ through its preferential interaction with the random coil state of Aβ. (Received Oct. 27, 2005; Accepted Dec. 3, 2005)

第51回低温生物工学会研究報告 12.
[Key words : Trehalose, β-amyloid, aggregation, Quartz Crystal Microbalance, Circular Dichroism spectroscopy ;トレハロース, β-アミロイド,凝集, 水晶発振子マイクロバランス法,円偏光二色性]

緒　　言

トレハロースは乾燥・凍結などの水ストレスに対して保護作用を示すだけでなく，不飽和脂肪酸に対する酸化抑制作用[1]，さらに最近ではハンチントン病原因蛋白質に対する凝集抑制作用[2]も見出されており，この糖の多彩な交差耐性効果が注目を集めている．おそらくトレハロースはタンパク質や細胞膜表面との直接的な相互作用を通してこれらの機能を発現すると思われるが，そのメカニズムについては不明な点が多い．本研究では，アルツハイマー病の異常蓄積タンパク質として知られている β-アミロイド(Aβ) をモデルに，トレハロースが凝集過程に及ぼす影響を調べることで，この糖が蛋白質構造に与える影響，蛋白質安定化作用について基礎的知見を得ることを目的とした．Aβ の凝集過程は複雑であり，Aβ 分子種，濃度，溶媒条件等の違いにより，オリゴマー，線維，ADDLs，プロトフィブリル，アミロスフェロイド等の様々な凝集体を形成する．そこで本研究では，特に初期凝集過程に対するトレハロースの影響を，水晶発振子マイクロバランス法(QCM)と円偏光二色性(CD)を用いて解析した．

材料および方法

QCM は，金基板上に固定したホスト分子に対する，測定系内に加えたゲスト分子の結合を発振子の振動数変化として検出するもので，結合過程を経時的に観測できる．(Fig.1)

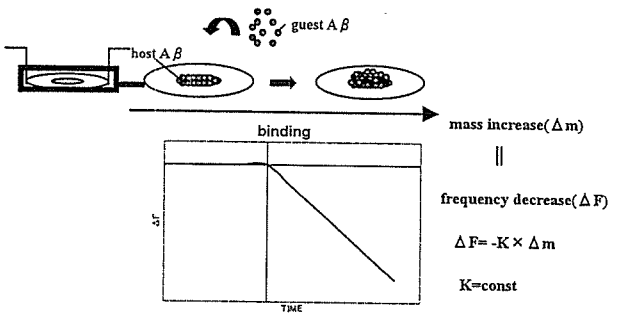

Fig. 1. Schematic diagram of QCM

本研究では，次の 3 つの系に対するトレハロース添加の効果を調べた．すなわち，①β シート構造の Aβ 同士の凝集，②基板上に固定した β シート構造の Aβ とランダムコイル構造の Aβ の凝集，③ランダムコイル構造の Aβ 同士の凝集である．比較対照として，ネオトレハロース，マルトースの添加実験も行った．まず，Aβ を QCM セルの基板に固定する．固定化法は系により 2 種類用いた．一つ目は，カチオン性の基板上に Aβ 溶液を滴下することで，中性付近で負に帯電している Aβ を静電的に固定する方法である．ここで，カチオン性基板は S 原子をもつ 2-アミノエタンチオール塩酸塩水溶液中に所定時間基板を浸漬させることにより作成した．もう一つの方法では、Aβ 溶液を所定時間基板と接触させることで，Aβ に含まれる S 原子と金基板を相互作用させて物理的に固定を行った．以上のいずれかの方法で Aβ を基板に固定した後，セルに溶媒 500μl を充填した．装置が安定化するのを待ち，二糖の溶液をセル内の濃度が 1mM となるよう測定系内に加え，装置付属の攪拌子で 5 秒間だけ攪拌した．さらに装置が安定化するのを待ち，Aβ 溶液を測定系内に加えて，測定を行った．この時の攪拌方法は Aβ 溶液を加えたときに数回ピペッティングする方法をとった．QCM 装置は株式会社イニシアム製 AFFINIX Q4 を用いた．Aβ は 40 残基の $Aβ_{1-40}$, 42 残基の $Aβ_{1-42}$ を用い，株式会社ペプチド研究所から購入した．これらは 70%アセトニトリル（株式会社メルク），0.05%トリフルオロ酢酸（株式会社ペプチド研究所）で凍結乾燥したのち使用直前に溶媒で 1mM になるよう溶解し，同じ溶媒で使用する濃度に希釈して用いた．溶媒として選択したリン酸緩衝生理食塩水(PBS)は日水製薬株式会社から，酢酸緩衝液の作製に使用した酢酸は和光純薬，酢酸ナトリウムは関東化学株式会社から購入した．トレハロース，ネオトレハロースは株式会社林原生物化学研究所から提供していただいた．マルトースは関東化学株式会社から購入した．①～③の各系に対する実験条件は Table 1 に示した．

次に，CD スペクトルを用いて溶液中の Aβ の二次構造を調べた．測定に使用した溶液は $Aβ_{1-40}$ の 30μM 溶液で，溶媒はリン酸緩衝生理食塩水 (pH 7.4) (PBS) である．トレハロースを加える場合，濃度は 1mM とした．CD 装置は (株) 日本分光製 J-720 spectropolarimeter，セルは光路長 0.1cm の石英製セル（GL サイエンス製）を用いた．

Table1. Experimental conditions of QCM measurements

		system①	system②	system③
Buffer		acetate buffer (pH 5.0)	acetate buffer (pH 5.0)	PBS (pH 7.4)
host Aβ		$Aβ_{1-42}$	$Aβ_{1-42}$	$Aβ_{1-40}$
	Secondary structure	β-sheet	β-sheet	random coil
	immobilization method	Physical	physical	electrostatic
	concentration	25μM	25μM	4μM
guest Aβ		$Aβ_{1-42}$	$Aβ_{1-40}$	$Aβ_{1-40}$
	Secondary structure	β-sheet	random coil	random coil
	concentration	10μM	1μM	1μM

結果および考察

Fig.1 で示した通り QCM の振動数変化と基板上の質量変化は比例関係にあり，振動数減少幅が大きいほど基板上の質量増大が大きいといえる．したがって，本研究のホストーゲスト系 system①～③において，基板上のホストへのゲスト分子の凝集が起こるならば，その進行にともない QCM の振動数減少が観測されるだろう．また，糖添加の効果は，一定時間経過後の振動数減少幅あるいは減少速度を比較することにより評価することができると考えられる．

Fig.2.a-c はそれぞれ system①～③に対する QCM 実験の結果を示す．各図において trehalose, neotrehalose, maltose はこれら二糖を添加した測定系の結果を示し，control は糖無添加系に対する結果を示す．

system①の糖無添加系では，約 150 分経過後 750Hz 程度の振動数減少が観測された．一方，トレハロース，ネオトレハロース，マルトースを添加系では，ほぼ同一時間経過後，それぞれ 670，750，540Hz 程度の振動数減少が観測された．したがって，ホスト，ゲストいずれも β シート構造 Aβ をもつ system①では，マルトースが最も高い凝集抑制効果を示すことが判明した．

それに対し system②では，150 分経過後の振動数減少幅は，糖無添加，トレハロース，ネオトレハロース，マルトースについて，それぞれ 390，200，410，310Hz であり，β シート構造の Aβ とランダムコイルの Aβ の凝集に関しては，トレハロースが最も高い凝集抑制効果をもつことが確認された．

興味あることに，ランダムコイル構造の Aβ 同士の凝集に対応する system③では，トレハロースを添加すると，糖無添加系に比べて振動数減少値が大きくなることが観測された．一方，ネオトレハロースとマルトースを添加した測定系では，system①と②の場合と同じく，糖無添加系に比べて振動数減少幅の減少が見られた．これらの結果は，ランダムコイル構造の Aβ 同士の凝集に関して，マルトースとネオトレハロースは凝集抑制効果をもつが，トレハロースはより重量の大きな凝集体形成を促進する効果をもつことを示している．しかし，この system③については実験ごとに値が変動するため，添加した Aβ の金基板への非特異的吸着などを再検討する必要もあることを付記しておく．

以上より，トレハロースの Aβ 凝集に対する効果として次の 2 つの特徴が見出された．すなわち，1）トレハロースが高い凝集抑制効果を示すのは，ホスト，ゲストのうち一方がランダムコイルのときである（system①と②の比較），2）ランダムコイル構造の Aβ 同士の凝集に対してトレハロースは他の二糖には無い特異的な効果をもつ（system③）．これらをまとめると，トレハロースはランダムコイル構造の Aβ に作用し，その凝集過程に有意な影響を与えると

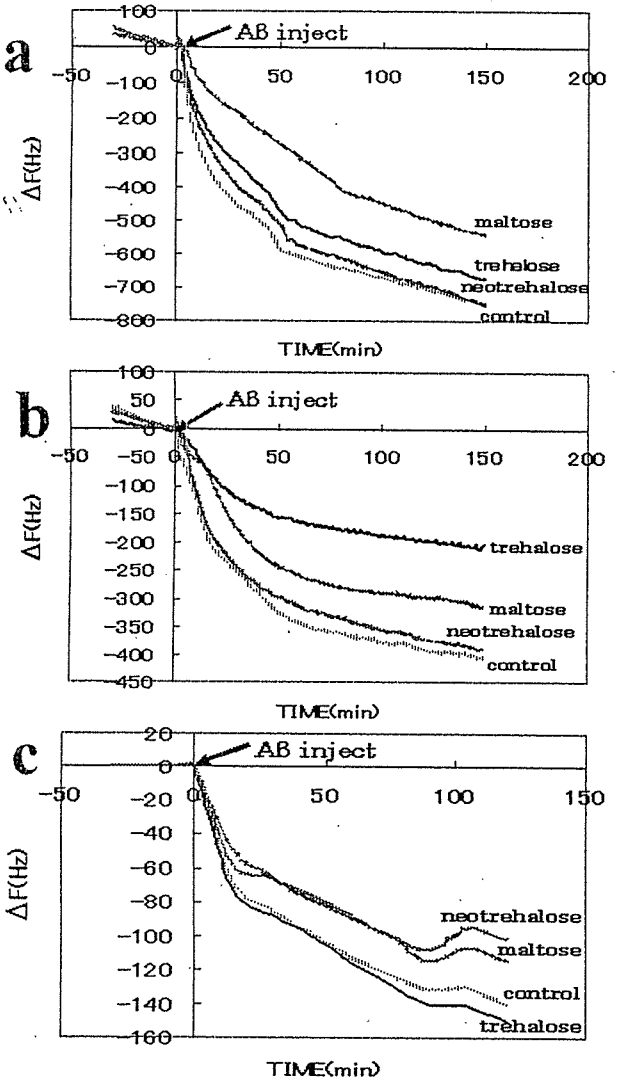

Fig. 2. Frequency shifts as a function of time during Aß aggregation

推定される.

そこで，トレハロースを添加した系と添加していない系それぞれに対して，Aβ がランダムコイル構造から β シート構造に変異するまでに要する時間を CD 測定より評価し比較した．トレハロースを添加していない系では，今回の測定条件においてランダムコイル構造から β シート構造への変異に要する時間が 190 時間だったのに対し，トレハロースを添加した系では 210 時間に延長されるこが確認できた．つまり，トレハロースは Aβ がランダムコイル構造から β シート構造への変異するのを抑制することが判明した．

ランダムコイル状態の Aβ では，親水基はもとより疎水基も水に露出していると考えられる．一方，最近のわれわれの研究によると，トレハロースは親水基のみならず，不飽和結合をもつ疎水基に特異的結合することが判明している[1,3]．これは他の二糖にはないトレハロース特有の性質である．したがって，system②や③の系では，トレハロースはおそらくランダムコイル Aβ の極性基のみならず疎水基とも水素結合を形成して安定化し，β シート構造への変異を抑制するとともに，凝集体の構造を変調しているのではないかと推測される．

謝　　辞

CD スペクトルの測定法をご指導してくださった東京工業大学大学院生命理工学研究科川崎剛美助手に深く感謝いたします．この研究は以下の研究費援助により行われた．本研究の一部は，生研センター基礎研究推進事業試験研究費（PROBRAIN）及び文部科学省科学研究費特定領域研究（no.16041212）により実施された．

文　　献

1) Oku, K., Watanabe, H., Kubota, M., Fukuda, S., Kurimoto,M., Tsujisaka, Y., Komori, M., Inoue, Y. and Sakurai, M. : NMR and quantum chemical study on the OH···π and CH···O interactions between trehalose and unsaturated fatty acids: J. Am. Chem. Soc., **125**, 12739-12748 (2003)

2) Tanaka, M., Machida, Y., Niu, S., Ikeda, T., Jana, R N.,Doi, H., Kurosawa, M., Nekooki, M. and Nukina, N.: Trehalose alleviates polyglutamine-mediated pathology in a mouse model of Huntington disease: Nature Med., **10**, 148-154 (2004)

3) Oku, M. Kurose, M., Kubota, S., Fukuda, M., Kurimoto, Y., Tujisaka, A., Okabe and Sakurai, M.: Combined NMR and quantum chemical study on the interaction between trehalose and diene relevant to the antioxidant function of trehalose, J. Phys. Chem. B, **109**, 3032-3040 (2005)

J|A|C|S
COMMUNICATIONS

Published on Web 11/23/2006

Design and Synthesis of an Enzyme Activity-Based Labeling Molecule with Fluorescence Spectral Change

Toru Komatsu,[†,§] Kazuya Kikuchi,[‡] Hideo Takakusa,[†] Kenjiro Hanaoka,[†] Tasuku Ueno,[†] Mako Kamiya,[†,§] Yasuteru Urano,[†,⊥] and Tetsuo Nagano*[,†,§]

Graduate School of Pharmaceutical Sciences, the University of Tokyo, 7-3-1, Hongo, Bunkyo-ku, Tokyo 113-0033, Japan, Graduate School of Engineering, Department of Material and Life Sciences, Osaka University, 2-1, Yamada-oka, Suita City, Osaka 565-0871, Japan, and CREST and PRESTO, JST Agency, Kawaguchi, Saitama, Japan

Received August 7, 2006; E-mail: tlong@mol.f.u-tokyo.ac.jp

Since proteins play central roles in a variety of cellular events, the study of protein dynamics is critical to an understanding of sophisticated processes of life. In recent years, chemistry-based strategies to modify, control, and monitor specific proteins have proved useful.[1−4] As represented by FlAsH that binds to a tetracysteine motif[5] and benzylguanine derivatives that bind to O^6-alkylguanine−DNA alkyltransferase,[6] techniques of covalent labeling of a specific tag protein with small-molecular dyes are effective for monitoring dynamic behaviors of proteins in living cells. However, one of the problems in monitoring protein dynamics with these techniques is the delay before detection of the target protein, owing to the need to wash out excess unreacted probe. It is desirable to develop a protein labeling technique that visualizes the process of the labeling reaction so that the labeled protein can be detected immediately at the point of labeling, that is, in the presence of unreacted probe.

In this paper, we describe a novel protein labeling probe that overcomes this problem by exhibiting a fluorescence wavelength change. With a probe whose fluorescence wavelength changes during the course of the labeling reaction, fluorescence of the labeled protein can be observed separately from that of the unreacted probe, so immediate detection and precise quantification of the target protein should be possible by monitoring the emission wavelength shift.

The design of the labeling reaction was based on quinone methide chemistry. Controlled formation and selective reaction of quinone methide have proved to be useful in chemically modifying cellular components such as nucleotides and proteins.[7−10] An advantage of this reaction is that formation of quinone methide entails bond scission, thereby changing the basic structure of the probe. In fluorescent probes based on fluorescence resonance energy transfer (FRET), structural change of the probe can be converted to a change of efficiency of FRET between two fluorophores.[11,12] The designed probe has two fluorophores that are expected to exhibit FRET, that is, 7-hydroxycoumarin as an energy donor and fluorescein as an energy acceptor. In the intact probe, these two fluorophores are positioned close to each other and FRET occurs efficiently. Upon labeling, the FRET efficiency decreases owing to loss of the donor fluorescein moiety as a leaving group. The change of FRET efficiency is reflected in an increase of fluorescence of the donor 7-hydroxycoumarin and a decrease of that of the acceptor fluorescein. By means of ratiometric measurement, the reaction rate can be monitored accurately.

Scheme 1. The Design of CMFβ-gal

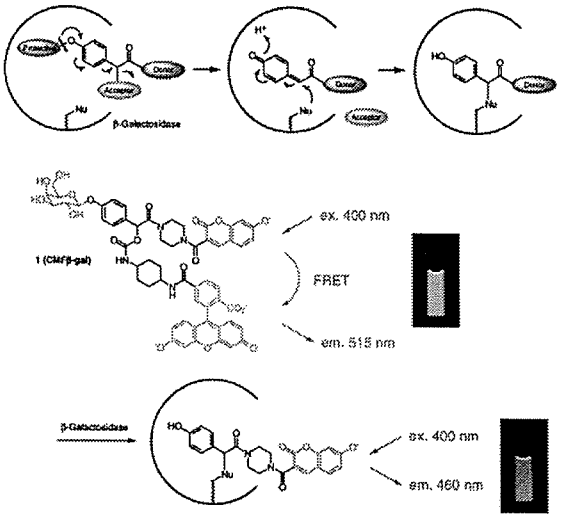

In quinone methide-forming molecules reported to date, halogens are mostly used as a leaving group,[7−10] but a leaving group with an appropriate structure is required for our purpose. This led us to design a probe with carbamate as a leaving group.

A good trigger for quinone methide formation is an enzymatic reaction that cleaves a phenol protective group to give a free phenol. We chose β-galactosidase from *Escherichia coli*, encoded by the *LacZ* gene,[13] as a target for labeling since its high turnover number for β-galactopyranosyl-protected phenols (1.8×10^5 s^{-1} for 2-nitrophenyl β-galactopyranoside[14]), its high substrate specificity for the glycon unit, and its wide tolerance for the aglycon unit are desirable features for a target of our probes.

The probe, named CMFβ-gal (coumarin−mandelate−fluorescein β-galactopyranosyl), was synthesized in 10 steps from commercially available 4-hydroxymandelic acid. As shown in the Supporting Information, a control compound CMfluorideβ-gal (coumarin−mandelate−fluoride β-galactopyranoside), with fluoride as a leaving group, was also synthesized for comparison of reactivity.

CMFβ-gal is stable in aqueous buffer solution (pH 7.4, 37 °C) for >24 h. The emission spectrum of CMFβ-gal in an aqueous buffer solution excited at 400 nm (peak excitation wavelength of 7-hydroxycoumarin) is shown in Figure 1.

Initially, emission of 7-hydroxycoumarin at around 460 nm was hardly observed, while a strong emission of fluorescein was seen at around 515 nm. This demonstrates that energy transfer proceeds efficiently in the intact probe, and FRET efficiency was calculated

[†] The University of Tokyo.
[‡] Osaka University.
[§] CREST.
[⊥] PRESTO.

10.1021/ja0657307 CCC: $33.50

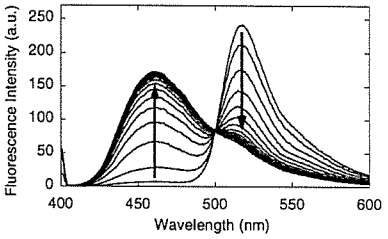

Figure 1. The emission spectra of a 1.0 μM solution of CMFβ-gal after the addition of β-galactosidase (11.6 $\mu g \cdot mL^{-1}$) in phosphate buffer (10 mM, pH 7.4) at 37 °C. The spectra were measured at every 4 min after the addition of β-galactosidase, λ_{ex} = 400 nm.

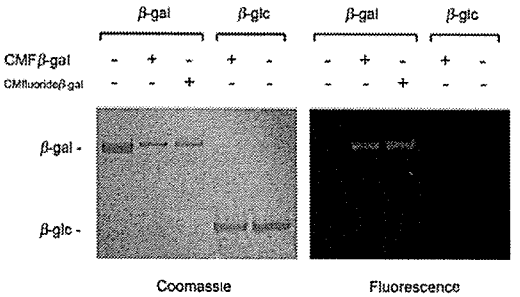

Figure 2. The result of SDS−PAGE (see Supporting Information for details of sample preparation). Left: image of Coomassie brilliant blue-stained gel. Right: fluorescence image of the gel under illumination at 365 nm from a UV lamp.

to be >93%. When β-galactosidase was added to the solution, a rapid increase in the emission of 7-hydroxycoumarin and a corresponding rapid decrease in the emission of fluorescein were observed. Monitoring of the increase of the ratio of fluorescence intensities at 460 and 515 nm allowed accurate estimation of the β-galactosidase concentration (see Supporting Information). After fluorescence change of reaction mixture had ceased, β-galactosidase was purified and its spectrum was measured to confirm that CMFβ-gal had indeed acted as a labeling probe of β-galactosidase. As shown in the Supporting Information, purified β-galactosidase exhibited the characteristic absorbance and fluorescence spectra of 7-hydroxycoumarin. These results were the same as that obtained with a control compound, CMfluorideβ-gal. In contrast, no labeling occurred when the probe was mixed with a control protein, β-glucosidase, instead of β-galactosidase. The labeled protein could also be detected with SDS−PAGE. As shown in Figure 2, fluorescence of 7-hydroxycoumarin was observed at the spot of β-galactosidase labeled with the probe, while it was not observed at the spot of β-glucosidase.

Finally, CMFβ-gal was used for ratiometric imaging in *LacZ*-positive or *LacZ*-negative cells to confirm that it can detect β-galactosidase expression in living cells (Figure 3). After microinjection of the probe, slight leakage occurred, but the increase in the emission of 7-hydroxycoumarin was clearly observed in *LacZ*-positive cells, while it was not apparent in *LacZ*-negative cells (see Supporting Information).

In conclusion, we have established a novel design strategy for quinone methide chemistry-based protein labeling probes, with carbamate as a leaving group. On the basis of this design, we

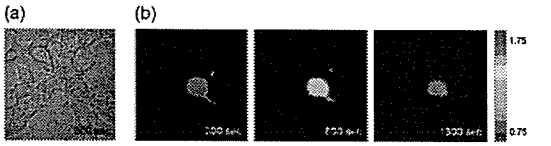

Figure 3. Bright-field transmission (a) and ratiometric images (b) of CMFβ-gal-injected *LacZ*-positive HEK293 cells at 300, 800, and 1300 s after microinjection. See Supporting Information for details.

synthesized a β-galactosidase labeling probe, CMFβ-gal, the labeling reaction of which can be monitored in terms of the change of fluorescence wavelength. This is the first report of a protein labeling probe which features a change of fluorescence wavelength upon reaction, allowing the labeled protein to be detected even in the presence of unreacted probe. The general probe design allows a wide tolerance in the selection of fluorophore pairs as well as protective groups for various enzymes. In applying this system to the other target enzymes, one possible limitation is that the feasibility of the labeling may depend on the structure of the protein, especially on the location of nucleophilic amino acids to be labeled.[9,10] Though, in future work, we think it would be possible to develop a range of probe and target enzyme pairs that serve as powerful tools in the study of protein dynamics in living cells.

Acknowledgment. We thank Haruhiko Bito and Hajime Fujii for technical support with SDS−PAGE. This work was financially supported by the Ministry of Education, Culture, Sports, Science and Technology of Japan (Grants for The Advanced and Innovational Research Program in Life Sciences, 16370071 and 16659003 to T.N., 15681012, 17651119, 17048006, 17035019, and 17036012 to K.K.). T.N. was also supported by the Hoh-ansha Foundation. K.K. was also supported by the Sankyo Foundation, by the Kanagawa Academy of Science, and by the Suzuken Memorial Foundation.

Supporting Information Available: Synthesis, experimental details, and characterization of CMFβ-gal and CMfluorideβ-gal, and additional experiments. This material is available free of charge via the Internet at http://pubs.acs.org.

References

(1) Tsien, R. Y. *Nat. Rev. Mol. Cell Biol.* **2003**, 16−21.
(2) Miller, L. W.; Cornish, V. W. *Curr. Opin. Chem. Biol.* **2005**, *9*, 56−61.
(3) Chen, I.; Ting, A. Y. *Curr. Opin. Biotechnol.* **2005**, *16*, 35−40.
(4) Yin, J.; Lin, A. J.; Buckett, P. D.; Wessling-Resnick, M.; Golan, D. E.; Walsh, C. T. *Chem. Biol.* **2005**, *12*, 999−1006.
(5) Griffin, B. A.; Adams, S. R.; Tsien, R. Y. *Science* **1998**, *281*, 269−272.
(6) Keppler, A.; Gendreizig, S.; Gronemeyer, T.; Pick, H.; Vogel, H.; Johnsson, K. *Nat. Biotechnol.* **2003**, *21*, 86−89.
(7) Halazy, S.; Danzin, C.; Ehrhard, A.; Gerhart, F. *J. Am. Chem. Soc.* **1989**, *111*, 3484−3485.
(8) Wang, Q.; Dechert, U.; Jirik, F.; Withers, S. G. *Biochem. Biophys. Res. Commun.* **1994**, *200*, 577−583.
(9) Janda, K. D.; Lo, L.-C.; Lo, C.-H.; Sim, M.-M.; Wang, R.; Wong, C.-H.; Lerner, R. A. *Science* **1997**, *275*, 945−948.
(10) Kurogochi, M.; Nishimura, S.; Lee, Y. C. *J. Biol. Chem.* **2004**, *279*, 44704−44712.
(11) Zlokarnik, G.; Negulescu, P. A.; Knapp, T. E.; Mere, L.; Burres, N.; Feng, L. X.; Whitney, M.; Roemer, K.; Tsien, R. Y. *Science* **1998**, *279*, 84−88.
(12) Takakusa, H.; Kikuchi, K.; Urano, Y.; Sakamoto, S.; Yamaguchi, K.; Nagano, T. *J. Am. Chem. Soc.* **2002**, *124*, 1653−1657.
(13) Horwitz, J. P.; Chua, J.; Curby, R. J.; Tomson, A. J.; Da Rooge, M. A.; Fisher, B. E.; Mauricio, J.; Klundt, I. *J. Med. Chem.* **1964**, *7*, 574−575.
(14) Feliu, J. X.; Villaverde, A. *FEBS Lett.* **1998**, *434*, 23−27.

JA0657307

J|A|C|S
ARTICLES
Published on Web 05/06/2006

Modulation of Luminescence Intensity of Lanthanide Complexes by Photoinduced Electron Transfer and Its Application to a Long-Lived Protease Probe

Takuya Terai,[†,‡] Kazuya Kikuchi,[§] Shin-ya Iwasawa,[†] Takao Kawabe,[∥] Yasunobu Hirata,[∥] Yasuteru Urano,[†,⊥] and Tetsuo Nagano*[,†,‡]

Contribution from the Graduate School of Pharmaceutical Sciences, The University of Tokyo, 7-3-1 Hongo, Bunkyo-ku, Tokyo 113-0033, Japan, CREST, JST, 4-1-8 Honcho, Kawaguchi, Saitama, 332-0012, Japan, Department of Material and Life Science, Division of Advanced Science and Biotechnology, Graduate School of Engineering, Osaka University, 2-1 Yamada-oka, Suita, Osaka, 565-0871, Japan, Department of Internal Medicine, Graduate School of Medicine, The University of Tokyo, 7-3-1 Hongo, Bunkyo-ku, Tokyo 113-0033, Japan, and PRESTO, JST, 4-1-8 Honcho, Kawaguchi-shi, Saitama, 332-0012, Japan

Received January 31, 2006; E-mail: tlong@mol.f.u-tokyo.ac.jp

Abstract: Luminescent lanthanide complexes (Tb^{3+}, Eu^{3+}, etc.) have excellent properties for biological applications, including extraordinarily long lifetimes and large Stokes shifts. However, there have been few reports of lanthanide-based functional probes, because of the difficulty in designing suitable complexes with a luminescent on/off switch. Here, we have synthesized a series of complexes which consist of three moieties: a lanthanide chelate, an antenna, and a luminescence off/on switch. The antenna is an aromatic ring which absorbs light and transmits its energy to the metal, and the switch is a benzene derivative with a different HOMO level. If the HOMO level is higher than a certain threshold, the complex emits no luminescence at all, which indicates that the lanthanide luminescence can be modulated by photoinduced electron transfer (PeT) from the switch to the sensitizer. This approach to control lanthanide luminescence makes possible the rational design of functional lanthanide complexes, in which the luminescence property is altered by a biological reaction. To exemplify the utility of our approach to the design of lanthanide complexes with a switch, we have developed a novel protease probe, which undergoes a significant change in luminescence intensity upon enzymatic cleavage of the substrate peptide. This probe, combined with time-resolved measurements, was confirmed in model experiments to be useful for the screening of inhibitors, as well as for clinical diagnosis.

Introduction

Sensitive detection of compounds of interest is one of the greatest challenges not only in analytical chemistry but also in biology and medicine. For decades, scientists have been developing a wide range of sophisticated spectroscopic approaches to address this issue. Fluorescence is one of the most widely used techniques in this field, because it offers many advantages, including sensitivity, simplicity, and robustness. From the early 1980s,[1] functional fluorescence probes have been developed, which change their fluorescence properties in response to their reaction with the chemical species of interest. Since they make possible a sensitive, safe, rapid, quantitative, and facile detection of the species both in vitro and in vivo, considerable attention has been devoted to the development of such probes, the targets of which include Ca^{2+},[1] Zn^{2+},[2] NO,[3] and enzymes.[4] These probes, however, have common disadvantages involving background fluorescence and scattered light. In the physiological environments such as cytoplasm and serum, sources of background fluorescence are present everywhere. Light scattering can also be a difficult problem when a conventional fluorescence probe, whose Stokes shift is only 20–30 nm, is used. These factors considerably impair the quality of measurements, especially when the scale of the assay is small or the probe concentration is low.

Luminescent lanthanide complexes[5] provide an attractive solution to these problems. If an appropriate chelator is used, a lanthanide (especially Tb^{3+} or Eu^{3+}) complex has an extraordinarily long luminescence lifetime of the order of milliseconds, in contrast to a typical organic compound, which has a short

† Graduate School of Pharmaceutical Sciences, The University of Tokyo.
‡ CREST, JST.
§ Osaka University.
∥ Graduate School of Medicine, The University of Tokyo.
⊥ PRESTO, JST.

(1) (a) Grynkiewicz, G.; Poenie, M.; Tsien, R. Y. *J. Biol. Chem.* **1985**, *260*, 3440–3450.
(2) Minta, A.; Kao, J. P. Y.; Tsien, R. Y. *J. Biol. Chem.* **1989**, *264*, 8171–8178.
(3) (a) Komatsu, K.; Kikuchi, K.; Kojima, H.; Urano, Y.; Nagano, T. *J. Am. Chem. Soc.* **2005**, *127*, 10197–10204. (b) Gee, K. R.; Zhou, Z. L.; Qian, W. J.; Kennedy, R. *J. Am. Chem. Soc.* **2002**, *124*, 776–778.
(4) Kojima, H.; Nakatsubo, N.; Kikuchi, K.; Kawahara, S.; Kirino, Y.; Nagoshi, H.; Hirata, Y.; Nagano, T. *Anal. Chem.* **1998**, *70*, 2446–2453.
(5) Mizukami, S.; Kikuchi, K.; Higuchi, T.; Urano, Y.; Mashima, T.; Tsuruo, T.; Nagano, T. *FEBS Lett.* **1999**, *453*, 356–360.

10.1021/ja060729t CCC: $33.50

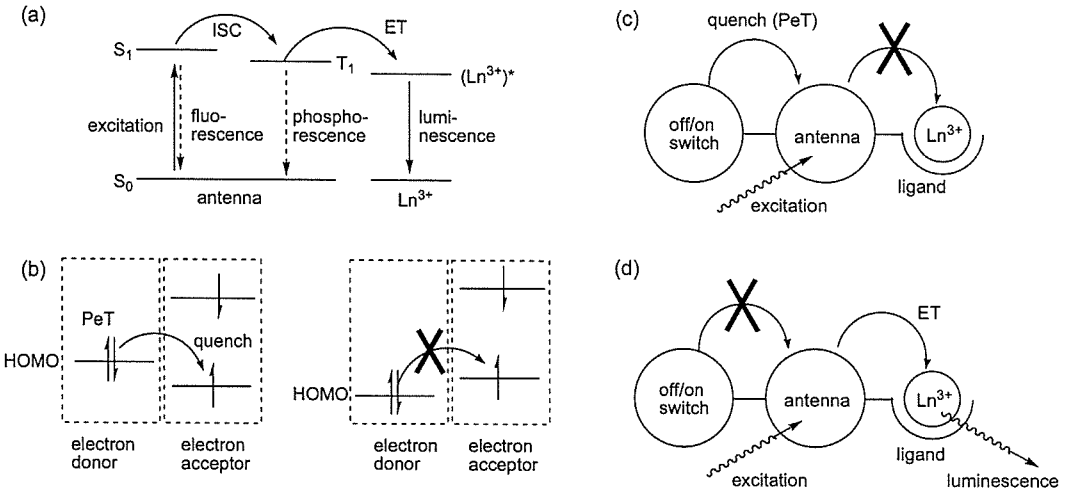

Figure 1. Schematic representations of our strategy to control the luminescence of lanthanide complexes. (a) Energy scheme for the luminescence process in a typical Ln^{3+} complex. (b) Schematic representation of the relationship between the HOMO energy level and photoinduced electron transfer. (c and d) Ln^{3+} complexes with a luminescence off/on switch. (c) Switch "off" model where PeT occurs, resulting in no Ln^{3+} luminescence. (d) Switch "on" model where PeT does not occur, resulting in strong Ln^{3+} luminescence.

fluorescence lifetime in the nanosecond region. Taking advantage of this feature, the influence of short-lived background fluorescence and scattered light can be reduced to a negligible level by the method termed time-resolved fluorescence (TRF) measurement.[6] In TRF measurement, the fluorescence signal is collected for a certain gate time after an appropriate delay time, following a pulsed excitation. By employing this method, it is readily possible to distinguish long-lived lanthanide luminescence from other contaminating signals. Furthermore, lanthanide complexes have large Stokes shifts (>200 nm), which also helps to reduce the background. Luminescent lanthanide complexes have been exploited as luminescent tags for TRF measurements in various fields,[7] especially immunoassays[8] and high throughput screenings,[9] where both high sensitivity and small assay scale are essential.

Since the lanthanide f−f transitions have a low absorption coefficient because of the Laporte selection rule, sensitized emission is often used to achieve high luminescence.[5] Here, a chromophore incorporated in the ligand (called a sensitizer or an antenna) absorbs excitation light with a large absorption coefficient and transfers its energy to the metal by intersystem crossing, whereby the metal enters the emission state (Figure 1a).[10] By choosing an appropriate antenna, it is possible to obtain a highly emissive lanthanide complex.[10a,11]

Currently, there is growing interest in lanthanide-based luminescence probes for biological applications. Compared with organic fluorophores, however, only a limited number of these probes have so far been reported, though their targets include pH,[12] cations,[13] anions,[14] and others.[15] The lack of a coherent strategy for the design of luminescent sensors slows the development of highly sensitive probes suitable for practical use.

Photoinduced electron transfer (PeT) is a comprehensively reported mechanism for excited-state quenching, in which an electron is transferred from an electron donor moiety to an

(6) (a) Parker, D.; Dickins, R. S.; Puschmann, H.; Crossland, C.; Howard, J. A. K. *Chem. Rev.* **2002**, *102*, 1977−2010. (b) Døssing, A. *Eur. J. Inorg. Chem.* **2005**, 1425−1434.

(7) (a) Hemmilá, I.; Mukkala, V.-M. *Crit. Rev. Clin. Lab. Sci.* **2001**, *38*, 441−519. (b) Lei, W.; Dürkop, A.; Lin, Z.; Wu, M.; Wolfbeis, O. S. *Microchim. Acta* **2003**, *143*, 269−274.

(8) (a) Selvin, P. R. *Annu. Rev. Biophys. Biomol. Struct.* **2002**, *31*, 275−302. (b) Lee, Y. C. *Anal. Biochem.* **2001**, *297*, 123−127. (c) Johansson, M. K.; Cook, R. M.; Xu, J.; Raymond, K. N. *J. Am. Chem. Soc.* **2004**, *126*, 16451−16455.

(9) (a) Yuan, J.; Wang, G.; Majima, K.; Matsumoto, K. *Anal. Chem.* **2001**, *73*, 1869−1876. (b) Mathis, G. *Clin. Chem.* **1993**, *39*, 1953−1959.

(10) (a) Hemmilä, I.; Webb, S. *Drug Discov. Today* **1997**, *9*, 373−381. (b) Karvinen, J.; Hurskainen, P.; Gopalakrishnan, S.; Burns, D.; Warrior, U.; Hemmilä, I. *J. Biomol. Screen.* **2002**, *7*, 223−231. (c) Préaudat, M.; Ouled-Diaf, J.; Alpha-Bazin, B.; Mathis, G.; Mitsugi, T.; Aono, Y.; Takahashi, K.; Takemoto, H. *J. Biomol. Screen.* **2002**, *7*, 267−274.

(11) (a) Alpha, B.; Lehn, J.-M.; Mathis, G. *Angew. Chem., Int. Ed. Engl.* **1987**, *26*, 266−267. (b) Beeby, A.; Faulkner, S.; Parker, D.; Williams, J. A. G. *J. Chem. Soc., Perkin Trans. 2* **2001**, 1268−1273. (11) (a) Li, M.; Selvin, P. R. *J. Am. Chem. Soc.* **1995**, *117*, 8132−8138. (b) Chen, J.; Selvin, P. R. *J. Photochem. Photobiol., A* **2000**, *135*, 27−32. (c) Steemers, F. J.; Verboom, W.; Reinhoudt, D. N.; van der Tol, E. B.; Verhoeven, J. W. *J. Am. Chem. Soc.* **1995**, *117*, 9408−9414. (d) Fu, L.-M.; Wen, X.-F.; Ai, X.-C.; Sun, Y.; Wu, Y.-S.; Zhang, J.-P.; Wang, Y. *Angew. Chem., Int. Ed.* **2005**, *44*, 747−750. (e) Dadabhoy, A.; Faulkner, S.; Sammes, P. G. *J. Chem. Soc., Perkin Trans. 2* **2002**, 348−357. (f) Petoud, S.; Cohen, S. M.; Bünzli, J.-C. G.; Raymond, K. N. *J. Am. Chem. Soc.* **2003**, *125*, 13324−13325. (g) Faulkner, S.; Pope, S. J. A. *J. Am. Chem. Soc.* **2003**, *125*, 10526−10527. (h) Mürner, H.-R.; Chasssat, E.; Thummel, R. P.; Bünzli, J.-C. G. *J. Chem. Soc., Dalton Trans.* **2000**, 2809−2816. (i) Coppo, P.; Duati, M.; Kozhevnikov, V. N.; Hofstraat, J. W.; De Cola, L. *Angew. Chem., Int. Ed.* **2005**, *44*, 1806−1810. (j) Galaup, C.; Carrié, M.-C.; Tisnès, P.; Picard, C. *Eur. J. Org. Chem.* **2001**, 2165−2175. (k) Elbanowski, S. L.; Mąkowska, B.; Hnatejko, Z. *J. Photochem. Photobiol., A* **2002**, *150*, 233−247.

(12) (a) de Silva, A. P.; Gunaratne, H. Q. N.; Rice, T. E. *Angew. Chem., Int. Ed. Engl.* **1996**, *35*, 2116−2118. (b) Parker, D.; Senanayake, P. K.; Williams, J. A. G. *J. Chem. Soc., Perkin Trans. 2* **1998**, 2129−2139. (c) Gunnlaugsson, T.; MacDónaill, D. A.; Parker, D. *J. Am. Chem. Soc.* **2001**, *123*, 12866−12876. (d) Lowe, M. P.; Parker, D.; Reany, O.; Aime, S.; Botta, M.; Castellano, G.; Gianolio, E.; Pagliarin, R. *J. Am. Chem. Soc.* **2001**, *123*, 7601−7609. (e) Gunnlaugsson, T.; Leonard, J. P.; Sénéchal, K.; Harte, A. J. *J. Am. Chem. Soc.* **2003**, *125*, 12062−12063.

(13) (a) de Silva, A. P.; Gunaratne, H. Q. N.; Rice, T. E.; Stewart, S. *Chem. Commun.* **1997**, 1891−1892. (b) Reany, O.; Gunnlaugsson, T.; Parker, D. *J. Chem. Soc., Perkin Trans. 2* **2000**, 1819−1831. (c) Hanaoka, K.; Kikuchi, K.; Kojima, H.; Urano, Y.; Nagano, T. *J. Am. Chem. Soc.* **2004**, *126*, 12470−12476.

(14) (a) Dickins, R. S.; Gunnlaugsson, T.; Parker, D.; Peacock, R. D. *Chem. Commun.* **1998**, 1643−1644. (b) Charbonnière, L.; Ziessel, R.; Montalti, M.; Prodi, L.; Zaccheroni, N.; Boehme, C.; Wipff, G. *J. Am. Chem. Soc.* **2002**, *124*, 7779−7788. (c) Atkinson, P.; Bretonniere, Y.; Parker, D. *Chem. Commun.* **2004**, 438−439.

(15) (a) de Sousa, M.; Kluciar, M.; Abad, S.; Miranda, M. A.; de Castro, B.; Pischel, U. *Photochem. Photobiol. Sci.* **2004**, *3*, 639−642. (b) Bobba, G.; Frias, J. C.; Parker, D. *Chem. Commun.* **2002**, 890−891. (c) Best, M. D.; Anslyn, E. V. *Chem.—Eur. J.* **2003**, *9*, 51−57. (d) Lee, K.; Dzubeck, V.; Latshaw, L.; Schneider, J. P. *J. Am. Chem. Soc.* **2004**, *126*, 13616−13617. (e) Hamblin, J.; Abboyi, N.; Lowe, M. P. *Chem. Commun.* **2005**, 657−659.

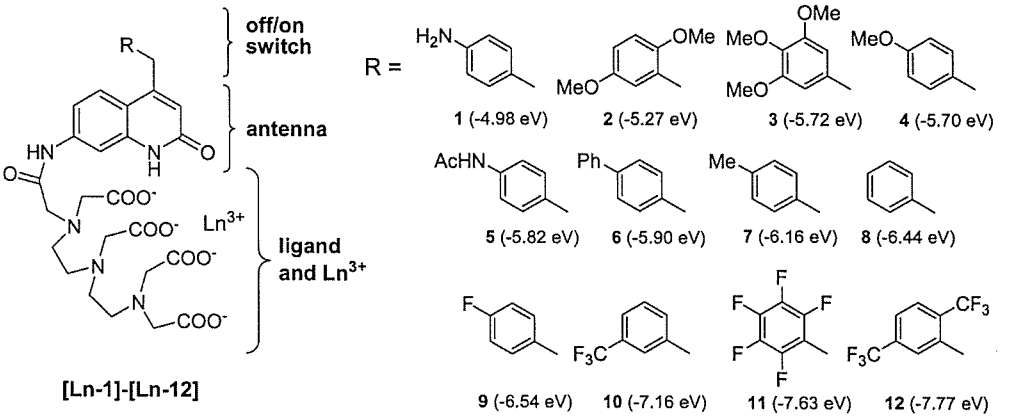

Figure 2. Structures of [Ln−1] to [Ln−12]. Calculated HOMO energy levels of the off/on switch moiety are also shown.

acceptor moiety.[16] If the electron donor has a high HOMO level, the fluorescence of the electron acceptor is quenched (Figure 1b). The PeT mechanism has been examined in detail as a fluorescence off/on switch for fluorescein derivatives,[17] and it has become possible to rationally develop fluorescein-based fluorescence probes with finely controlled photophysical properties.[18]

In the case of lanthanide complexes, PeT can take place in several ways: ligand to metal,[19] ligand to ligand,[12a,15a,20] extramolecular species to metal or ligand,[21] and others. Among them, intramolecular PeT within the ligand moiety should be most useful in rationally developing a luminescence probe, because using this kind of PeT as a switch eliminates the need to incorporate the reactive moiety in the antenna, which is a great limitation in designing a probe. In other words, it is possible to optimize the reactive moiety for the target species independently of the antenna structure. Surprisingly, this sort of PeT has not been investigated in detail before.

With the aim of establishing a rational and convenient methodology for the development of long-lived luminescence probes, we set out to scrutinize the potent role of PeT within the ligand moiety as a luminescence off/on switch. We have synthesized a series of complexes, **[Ln−X]** (**Ln = Eu, Tb**) (**X = 1−12**), the ligands of which consist of three moieties: a chelator, an antenna, and a luminescence on/off switch, of which the latter corresponds to the reactive moiety of the probe. Clear dependence of lanthanide luminescence on the switch HOMO level was observed, which shows that the luminescence intensity of the lanthanide complexes can indeed be controlled by intramolecular PeT within the ligand.

To demonstrate the feasibility of the PeT-based design of luminescence probes, a novel luminescence probe, **[Ln−13]** (**Ln = Tb, Eu**), for a protease, microsomal leucine aminopeptidase (LAP), was developed. This complex drastically changes its luminescence property in response to the enzymatic activity of LAP. Applications of the probe for inhibition activity assay, microplate assay, and clinical diagnosis are described. To our knowledge, this is the first functional long-lived luminescence probe for enzymatic activity, controlled by the PeT mechanism.

Results and Discussion

Design and Synthesis of [Ln−X]. To examine the effect of PeT within the ligand moiety, we designed and synthesized a series of complexes **[Ln−X]** (**Ln = Eu, Tb**) (**X = 1−12**), which consist of three parts: a Ln^{3+} chelate, an antenna, and a luminescence on/off switch (Figure 2). As a chelator, diethylenetriaminepentaacetic acid (DTPA) was chosen. DTPA forms a highly stable ($K_{ML} = 10^{22.39}$ and $10^{22.71}$ for Eu^{3+} and Tb^{3+}, respectively)[22] complex with a Ln^{3+} ion, with a coordination number of 8.[23]

It also prevents solvent water molecules from coupling away energy from the excited state of the lanthanide ion. As an antenna, 7-amino-4-methyl-2(1*H*)-quinolinone (cs124) was selected, because the DTPA-amide of this compound works as an efficient sensitizer for both Tb^{3+} and Eu^{3+} in aerated water.[11a,24] The luminescence on/off switch is a substituted benzene of appropriate electron density, which was linked to the methyl group of the antenna to avoid conjugative coupling of the two aromatic rings. We have synthesized 12 compounds as described in detail in the Supporting Information, followed by complexation with Ln^{3+}.

Calculation of HOMO Energy Level. The likelihood of PeT can be judged from the change in free energy (ΔG_{eT}), which is calculated from the Rehm−Weller eq 1

$$\Delta G_{eT} = E_{ox} - E_{red} - \Delta E_{0,0} - w_p \qquad (1)$$

where E_{ox} and E_{red} are the oxidation and reduction potentials of the electron donor (on/off switch moiety) and acceptor

(16) Callan, J. F.; de Silva, A. P.; Magri, D. C. *Tetrahedron* **2005**, *61*, 8551−8588.
(17) (a) Ueno, T.; Urano, Y.; Setukinai, K.; Takakusa, H.; Kojima, H.; Kikuchi, K.; Ohkubo, K.; Fukuzumi, S.; Nagano, T. *J. Am. Chem. Soc.* **2004**, *126*, 14079−14085. (b) Miura, T.; Urano, Y.; Tanaka, K.; Nagano, T.; Ohkubo, K.; Fukuzumi, S. *J. Am. Chem. Soc.* **2003**, *125*, 8666−8671.
(18) (a) Kenmoku, S.; Urano, Y.; Kanda, K.; Kojima, H.; Kikuchi, K.; Nagano, T. *Tetrahedron* **2004**, *60*, 11067−11073. (b) Urano, Y.; Kamiya, M.; Kanda, K.; Ueno, T.; Hirose, K.; Nagano, T. *J. Am. Chem. Soc.* **2005**, *127*, 4888−4894. (c) Kamiya, M.; Urano, Y.; Ebata, N.; Yamamoto, M.; Kosuge, J.; Nagano, T. *Angew. Chem., Int. Ed.* **2005**, *44*, 5439−5441.
(19) (a) Abu-Saleh, A.; Meares, C. F. *Photochem. Photobiol.* **1984**, *39*, 763−769. (b) Aime, S. et al. *J. Chem. Soc., Dalton Trans.* **1997**, 3623−3636. (c) Dickins, R. S.; Howard, J. A. K.; Maupin, C. L.; Moloney, J. M.; Parker, D.; Riehl, J. P.; Siligardi, G.; Williams, J. A. G. *Chem.−Eur. J.* **1999**, *5*, 1095−1105.
(20) Parker, D. *Coord. Chem. Rev.* **2000**, *205*, 109−130.
(21) Poole, R. A.; Bobba, G.; Cann, M. J.; Frias, J.-C.; Parker, D.; Peacock, R. D. *Org. Biomol. Chem.* **2005**, *3*, 1013−1024.
(22) Moeller, T.; Thompson, L. C. *J. Inorg. Nucl. Chem.* **1962**, *24*, 499−510.
(23) Caravan, P.; Ellison, J. J.; McMurry, T. J.; Lauffer, R. B. *Chem. Rev.* **1999**, *99*, 2293−2352.
(24) Selvin, P. R.; Jancarik, J.; Li, M.; Hung, L.-W. *Inorg. Chem.* **1996**, *35*, 700−705.

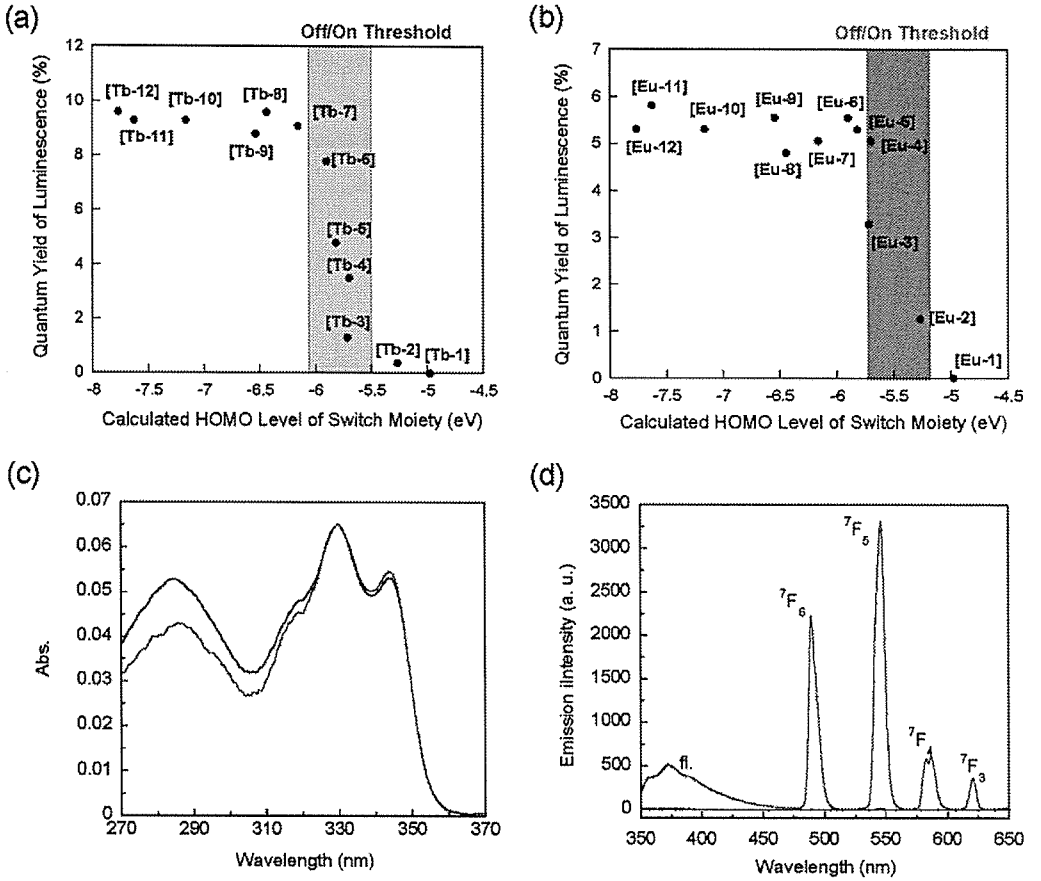

Figure 3. Spectroscopic properties of **[Ln−X]**. Plot of luminescence intensity as a function of the calculated HOMO level of the switch moiety in the cases of (a) Tb^{3+} and (b) Eu^{3+} complexes. (c) Absorption and (d) emission spectra of **[Tb−8]** (green line) and **[Tb−1]** (black line) 5 μM in aqueous solution (100 mM HEPES buffer, pH 7.3, I = 0.1 ($NaNO_3$)). Excitation wavelength was 330 nm. The attribution of each band is shown in the figure (see text).

(antenna moiety), $\Delta E_{0,0}$ is the singlet excited energy, and w_p is the work term for the charge separation state.[25] If a fixed acceptor is used, low E_{ox} leads to a negative Δ_{eT} value and facilitates the electron transfer, as can easily be understood from eq 1. Hence, the fluorescence intensity of the compound primarily depends on the oxidation potential of the electron donor moiety. This parameter can be readily evaluated from the HOMO energy level of the donor moiety, as shown for fluorescein derivatives.[18a,b]

Our working hypothesis was that the strategy used in fluorescein derivatives would also be applicable to the synthesized lanthanide complexes **[Ln−X]**. We anticipated that, provided that the HOMO level of the switch moiety is high enough to induce PeT to the antenna, the singlet excited state of the antenna would be quenched, resulting in no luminescence from Ln^{3+} (Figure 1c). In contrast, a complex with a switch having a low HOMO level would not suffer from this quenching mechanism and would emit strong luminescence (Figure 1d).

Bearing this in mind, the HOMO energy level of the luminescence on/off switch of **1**−**12** was calculated by the DFT method using the B3LYP/6-31G(d) basis set. The results are shown in Figure 2. The values cover a wide range from −4.98 eV of **1** to −7.77 eV of **12**.

(25) Rehm, D.; Weller, A. *Isr. J. Chem.* **1970**, *8*, 259−271.

Photochemical Properties of [Ln−X]. For each synthesized complex, the quantum yield of luminescence in neutral aqueous buffer was determined and plotted against the calculated HOMO energy level of the switch moiety (Figure 3). As expected, a clear dependence of quantum yield on the HOMO level was observed for both Tb^{3+} and Eu^{3+} complexes. The threshold level of luminescence on and off switching was shown to be around −5.8 eV for Tb and −5.5 eV for Eu. Only the complexes with a HOMO level of the switch moiety below the threshold have strong luminescence, and their quantum yields are similar to those of the complexes without the switch moiety (12.1% and 4.3% for Tb^{3+} and Eu^{3+} complexes, respectively). The slight difference of the threshold level between Tb^{3+} and Eu^{3+} is probably due to the effect of the metal on the π-system of the antenna moiety. Such a phenomenon has been suggested before in a complex in which the antenna directly binds to the lanthanide ion.[12a] Considering that the 7-amide group of cs124-DTPA-Ln is known to participate in metal binding,[24] our result is not surprising.

To scrutinize the mechanism of quenching, the luminescence and chemical properties of **[Ln−X]** were investigated. For clarity, the absorption and emission spectra of **[Tb−8]** (PeT off state) and **[Tb−1]** (PeT on state) are shown in Figure 3c and 3d, respectively. The UV−vis absorption spectra (over

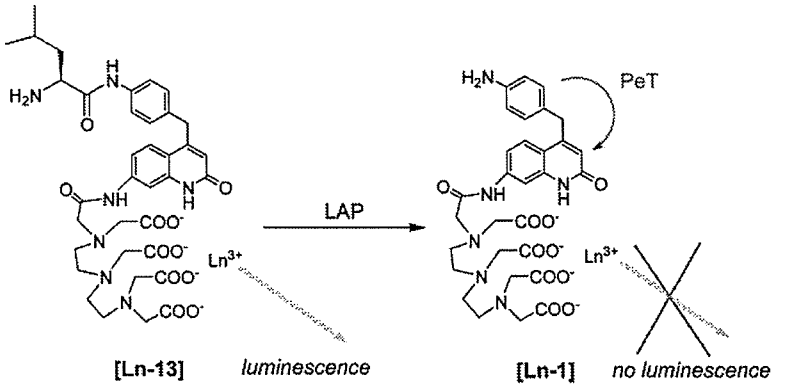

Figure 4. Schematic representation of the probe. **Ln = Tb, Eu.**

310 nm) did not change among the complexes, showing that the ground state of the antenna is not affected by the switch moiety. For **[Tb-8]**, short-lived emission of the antenna moiety (labeled as fl. in Figure 3d) was detected at around 370 nm, as well as four luminescence bands of Tb^{3+} at 490, 546, 583, and 621 nm. These bands correspond to the transition from the $^5D_4$ excited state to the $^7F_6$, $^7F_5$, $^7F_4$, and $^7F_3$ ground state, respectively. No emission, however, was observed from **[Tb−1]**, including the fluorescence of the antenna at around 370 nm. In the case of Eu^{3+} complexes, essentially identical results were obtained, except that the observed transition from the Eu^{3+} excited state occurred from $^5D_0$ to ^7F_J ($J = 0, 1, 2, 3, 4$) (Figure S1). This quenching of antenna fluorescence, in cooperation with the luminescence from Ln^{3+}, indicates a presence of a quenching pathway, such as PeT, to the singlet excited state of the antenna moiety.

Other parameters listed in Table S1 (Tb^{3+} complexes) and S2 (Eu^{3+} complexes) are also consistent with the idea that the luminescence of **[Ln−X]** is controlled by PeT from the off/on switch moiety to the antenna singlet state. The triplet energy level of the antenna, calculated from the phosphorescence spectra measured in MeOH/EtOH = 1:1 at 77 K did not change at all, which excludes the possibility that the quenching of luminescence is due to a change of the nature of the antenna triplet state. In addition, either in H_2O or in D_2O, the luminescence lifetimes of the complexes with different switches did not vary, demonstrating that the excited state of the lanthanide ion remains intact. It is well-known that the O−H oscillator of solvent coordinated to the metal center can quench the luminescence from Ln^{3+}.[26,27] For every complex, however, the number of coordinated water molecules (q values) at the metal center was estimated to be approximately 1, using the equation proposed by Parker et al.[27] This shows that the off/on switch does not change this nonradiative decay of Ln^{3+} by bound water molecules.

Figure 3a and 3b provide us with highly significant information for designing a luminescence probe. To develop a practical probe with a large change of luminescence in response to the target, what we need to do is to find a reactive moiety whose HOMO level is changed across the threshold by the reaction. In other words, we can screen and optimize the structure of the probe *in silico*. Compared with the previously exploited *trial and error* approach, this rational method should have many advantages, including savings of cost and time.

Design and Photochemical Properties of an LAP Probe. Based on the above findings, we set out to develop a protease probe based on PeT. A protease is an enzyme which cleaves a specific peptide bond of a substrate peptide or protein. There are enormous numbers of enzymes in this category,[28] many of which are related to various diseases.[29] Although several protease substrates for chromogenic and fluorogenic assays have been reported,[30] none of them has a long-lived luminescence except for a few[31] based on RET (resonance energy transfer). In contrast to RET-based probes, which require two chromophores at appropriate sites, probes using PeT should provide simple and robust assays and should also be applicable to exopeptidases.

Among the proteases, microsomal leucine aminopeptidase (LAP) was selected as the target enzyme. LAP (EC 3.4.11.2, also known as aminopeptidase M or aminopeptidase N) is a widespread exopeptidase, which removes N-terminal amino acids (preferably leucine and alanine) from almost all unsubstituted oligopeptides.[28] It is well-known that LAP plays important roles in tumor-cell invasion,[32] tumor metastasis,[33] and maturation of MHC class I epitopes.[34] Although chromogenic and fluorogenic substrates, L-pNA[35] and L-MCA,[36]

(26) Horrocks, W. DeW., Jr.; Sudnick, D. R. *Acc. Chem. Res.* **1981**, *14*, 384−392.
(27) Beeby, A.; Clarkson, I. M.; Dickins, R. S.; Faulkner, S.; Parker, D.; Royle, L.; de Sousa, A. S.; Williams, J. A. G.; Woods, M. *J. Chem. Soc., Perkin Trans. 2* **1999**, 493−503.
(28) Barrett, A. J.; Rawlings, N. D.; Woessner, J. F. *Handbook of Proteolytic Enzymes*, 2nd ed.; Elsevier Academic Press: Amsterdam, The Netherlands, 2004.
(29) (a) Southan, C. *Drug Discov. Today* **2001**, *6*, 681−688. (b) Artal-Sanz, M.; Tavernarakis, N. *FEBS Lett.* **2005**, *579*, 3287−3296. (c) Singh, R. B.; Dandekar, S. P.; Elimban, V.; Gupta, S. K.; Dhalla, N. S. *Mol. Cell. Biochem.* **2004**, *263*, 241−256.
(30) (a) Erlanger, B. F.; Kokowsky, N.; Cohen, W. *Arch. Biochem. Biophys.* **1961**, *95*, 271−278. (b) Zimmerman, M.; Yurewicz, E.; Patel, G. *Anal. Biochem.* **1976**, *70*, 258−262. (c) Leytus, S. P.; Patterson, W. L.; Mangel, W. F. *Biochem. J.* **1983**, *215*, 253−260.
(31) (a) Karvinen, J.; Elomaa, A.; Mäkinen, M.-L.; Hakala, H.; Mukkala, V.-M.; Peuralahti, J.; Hurskainen, P.; Hovinen, J.; Hemmilä, I. *Anal. Biochem.* **2004**, *325*, 317−325.(b) Karvinen, J.; Laitala, V.; Mäkinen, M.-L.; Mulari, O.; Tamminen, J.; Hermonen, J.; Hurskainen, P.; Hemmilä, I. *Anal. Chem.* **2004**, *76*, 1429−1436.
(32) Saiki, I.; Fujii, H.; Yoneda, J.; Abe, F.; Nakajima, M.; Tsuruo, T.; Azuma, I. *Int. J. Cancer* **1993**, *54*, 137−143.
(33) Fujii, H.; Nakajima, M.; Saiki, I.; Yoneda, J.; Azuma, I.; Tsuruo, T. *Clin. Exp. Metastasis* **1995**, *13*, 337−344.
(34) Saric, T.; Chang, S.-C.; Hattori, A.; York, I. A.; Markant, S.; Rock, K. L.; Tsujimoto, M.; Goldberg, A. L. *Nat. Immunol.* **2002**, *3*, 1169−1176.
(35) Tuppy, H.; Wiesbauer, U.; Wintersberger, E. *Hoppe-Seyler's Z. Physiol. Chem.* **1962**, *329*, 278−288.
(36) Kanaoka, Y.; Takahashi, T.; Nakayama, H. *Chem. Pharm. Bull.* **1977**, *25*, 362−363.
(37) Melhuish, W. H. *J. Phys. Chem.* **1961**, *65*, 229−235.

Table 1. Photochemical Properties of the Probes

	abs_{max} (nm)	ϵ	em_{max} (nm)	Φ_{lum}[a] (%)	τ_{H_2O} (ms)	τ_{D_2O} (ms)	q[b]
[Tb−13]	330	13 000	547	6.8	1.12	1.70	1.20
[Tb−1]	330	13 000	547	0.01	n.d.[c]	n.d.[c]	n.d.[c]
[Eu−13]	330	13 000	614	4.8	0.62	2.10	0.96
[Eu−1]	330	13 000	614	0.01	n.d.[c]	n.d.[c]	n.d.[c]

[a] Quantum yields were determined using quinine sulfate ($\Phi = 0.546$ in 1 N H_2SO_4)[37] for Tb and $[Ru(bpy)_3]Cl_2$ ($\Phi = 0.028$ in air-equilibrated water)[38] for Eu complexes as standards. Measurements were performed in 100 mM HEPES buffer (pH 7.4) at 25 °C. [b] q values were estimated using the equation $q = 5(\tau_{H_2O}^{-1} - \tau_{D_2O}^{-1} - 0.06)$ (for Tb) and $q = 1.2(\tau_{H_2O}^{-1} - \tau_{D_2O}^{-1} - 0.25 - 0.075)$ (for Eu).[27] [c] Not determined.

respectively, have been reported, there is so far no substrate suitable for TRF measurement.

The design of the probe is shown in Figure 4. The substrate peptide sequence of LAP, L-Leu, was attached through a peptide bond to the amino group of the luminescence off/on switch moiety of **[Ln−1]** (for detailed synthetic procedure, see Supporting Information). The synthesized compound, **[Ln−13]**, was expected to have strong luminescence, because the HOMO energy level of its switch moiety (−5.89 eV) was similar to that of **[Ln−6]**. After the cleavage of the peptide by LAP, **[Ln−13]** would be converted to **[Ln−1]**, whose luminescence would be quenched by PeT.

The photochemical properties of **[Ln−13]**, compared with those of **[Ln−1]**, were summarized in Table 1. As expected, the parameters do not differ from each other except for the quantum yields of luminescence. The quantum yields of **[Ln−13]** were close to those of **[Ln−6]**, indicating the accuracy of the prediction from the calculated HOMO energy level. For both Tb^{3+} and Eu^{3+}, the luminescence intensity of the complexes before and after the LAP-mediated reaction differed by approximately 500-fold, indicating that this probe is potentially useful for the sensitive detection of LAP activity. Because the quantum yield of **[Tb−13]** is higher than that of the corresponding Eu^{3+} complex, most of the following experiments were performed with **[Tb−13]**.

Enzymatic Reaction and Assessment of Inhibitory Activity. When the probe was reacted with LAP, the emission from Ln^{3+}, as well as that from the antenna, decreased in a time-dependent manner (Figure 5) until complete quenching was achieved (Figure S2). This decrease was not observed if the enzyme was absent or if the **[Ln−13]** complex was replaced with **[Ln−5]** (Figure S3). In addition, other proteases, such as trypsin, chymotrypsin, elastase, caspase-3, and cathepsin B, did not affect the luminescence of the probe (for trypsin, data are shown in Figure S3), which shows that **[Ln−13]** is a specific probe for LAP activity. The conversion of **[Tb−13]** to **[Tb−1]** was confirmed by analytical HPLC (Figure S4).

Kinetic parameters of **[Tb−13]** were determined and compared with those of commercially available substrates, L-pNA and L-MCA (Table S3). The K_m and k_{cat} of **[Tb−13]** were found to be 4.18×10^5 M and 29.3 s^{-1}, respectively. The k_{cat}/K_m value was 7.01×10^5 (M^{-1} s^{-1}), virtually identical with those of L-pNA and L-MCA (7.17×10^5 and 6.13×10^5 M^{-1} s^{-1}). This result indicates that the reaction rates are almost the same, when the probe concentration is low.

One possible application of a spectroscopic probe for a protease is to evaluate inhibitory activities of candidate compounds. Indeed, protease inhibitors are widely used as therapeutic drugs.[39] In particular, LAP inhibitors are suggested to have antitumor angiogenesis activity.[39b] Thus, we have investigated the applicability of **[Tb−13]** for the assessment of inhibitory activity. Several compounds are known to inhibit the activity of LAP, including actinonin,[40] amastatin,[41] and bestatin.[42] The inhibitory activities of these three inhibitors were probed with L-pNA, L-MCA, and **[Tb−13]**, respectively, and the inhibition constants K_i were determined on the assumption that these inhibitors were noncompetitive (Table S4).[43] Similar results were obtained regardless of the probes used.

TRF Assay on Microplate. Microplates (96-well, 384-well, etc.) are an indispensable tool for biological and environmental assays. They can handle a large number of samples simultaneously with a small sample volume (microliter order) and are suitable for automated assay systems. They are, however, more likely to suffer from autofluorescence of the device and scattered light. Therefore, TRF measurements with low background signals are expected to be highly advantageous compared with the use of organic fluorescent compounds.[9a,44]

After confirming that LAP activity on a 96-well plate could be monitored with 2.5 μM **[Tb−13]** by TRF measurement (Figure S5), we conducted experiments with lower concentrations of **[Tb−13]**, such as at nanomolar level. The experiments were repeated using L-MCA to compare the results. At 50 nM, **[Tb−13]** could clearly detect the presence of inhibitor ($P < 0.001$ by Student's t-test), while L-MCA failed to show a statistically significant difference of fluorescence intensity ($P > 0.05$) between with and without inhibitor, due to the large background signal (Figure 6).

We also performed experiments with smaller amounts of LAP. With **[Tb-13]**, as little as 1 μU of LAP could be detected (Figure S6a) in a concentration-dependent manner. With L-MCA, however, no increase of fluorescence intensity was observed when the amount of LAP was lower than 50 μU, presumably due to the influence of the background signal (Figure S6b).

Although some influence of the apparatus cannot be excluded, these results suggest that TRF measurements with **[Tb-13]** offer higher reproducibility and sensitivity than conventional fluorescence assays in a system with a high background signal level, such as microplates.

Application for Clinical Diagnosis. LAP is a clinically significant enzyme, and elevated levels of LAP activity in serum are associated with diseases of the liver, bile duct, and pancreas.[45] As LAP activity in serum renders valuable information for clinical diagnosis, it is often quantified in hospitals. To

(38) Nakamaru, K. *Bull. Chem. Soc. Jpn.* **1982**, *55*, 2697−2705.

(39) (a) Leung, D.; Abbenante, G.; Fairlie, D. P. *J. Med. Chem.* **2000**, *43*, 305−341.(b) Aozuka, Y.; Koizumi, K.; Saitoh, Y.; Ueda, Y.; Sakurai, H.; Saiki, I. *Cancer Lett.* **2004**, *216*, 35−42.

(40) Umezawa, H.; Aoyagi, T.; Tnanaka, T.; Suda, H.; Okuyama, A.; Naganawa, H.; Hamada, M.; Takeuchi, T. *J. Antibiotics* **1985**, *38*, 1629−1630.

(41) Aoyagi, T.; Tobe, H.; Kojima, F.; Hamada, M.; Takeuchi, T.; Umezawa, H. *J. Antibiotics* **1978**, *31*, 636−638.

(42) Umezawa, H.; Aoyagi, T.; Suda, H.; Hamada, M.; Takeuchi, T. *J. Antibiotics* **1976**, *29*, 97−99.

(43) Barclay, R. K.; Phillips, M. A. *Biochem. Biophys. Res. Commun.* **1980**, *96*, 1732−1738.

(44) Gudgin Dickson, E. F.; Pollak, A.; Diamandis, E. P. *J. Photochem. Photobiol., B* **1995**, *27*, 3−19.

(45) (a) Szasz, G. *Am. J. Clin. Path.* **1967**, *47*, 607−613. (b) Shay, H.; Sun, D. C. H.; Siplet, H. *Am. J. Digest. Dis.* **1960**, *5*, 217−232. (c) Pineda, E. P.; Goldbarg, J. A.; Banks, B. M.; Rutenburg, A. M. *Gastroenterology* **1960**, *38*, 698−712.

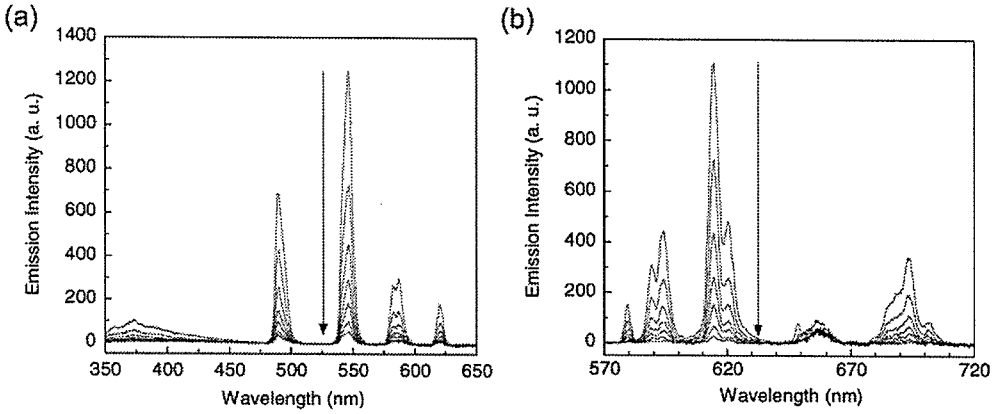

Figure 5. Reaction of **[Ln−13]** with LAP. Emission spectra of 2 μM (a) **[Tb−13]** and (b) **[Eu−13]** at 0, 5, 10, 15, 20, 30, and 60 min after the addition of LAP (0.01 U). The reaction was performed in 100 mM Tris-HCl buffer (pH 7.4) at 37 °C. The excitation wavelength was 330 nm.

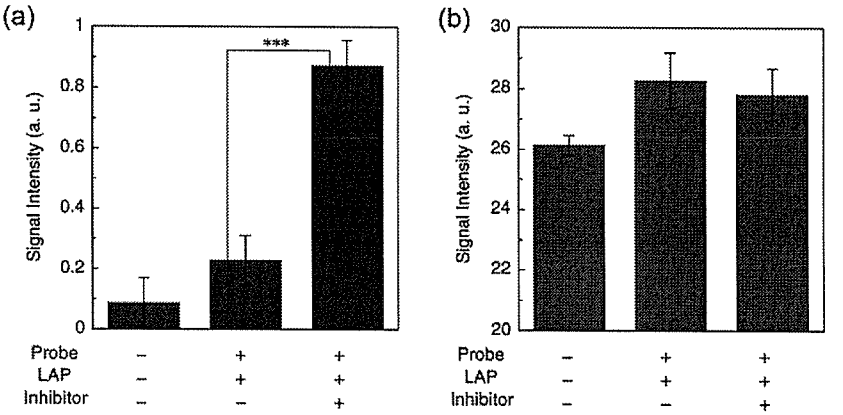

Figure 6. Microplate assay of LAP (0.002 U) with 50 nM (a) **[Tb−13]** (TRF measurement) and (b) L-MCA. Amastatin (10 μM) was added as an inhibitor. Fluorescence intensity (ex./em. = 325/545 nm for (a) and 380/440 nm for (b)) was recorded 60 min after the initiation of the reaction. Data are shown as mean ± SEM (n = 5). *** indicates $P < 0.001$.

examine the feasibility of applying **[Tb-13]** for clinical diagnosis, we conducted experiments using human sera. This is a challenging experimental condition, since serum contains hundreds of biological compounds and ions. It absorbs more than 90% of excitation light (at 330 nm), emitting a strong background fluorescence. Using TRF measurements, LAP activities in sera were quantified in both normal volunteers and patients with cancer (5 persons each). As can be seen in Figure 7, LAP activity was 1.9-fold higher in sera from patients than in sera from normal persons ($P < 0.01$ by Student's t-test). The results obtained with this method were shown to have a high linear correlation (r = 0.94) with commercially performed measurements of the same samples, conducted with a chromogenic substrate (Figure S7). Moreover, the coefficient of variation (CV) for normal patients was 17.7, about half that of the chromogenic method (30.0). The luminescence intensity of **[Tb−13]** did not change at all when amastatin, a known inhibitor of LAP, was added to the serum, which confirmed that **[Tb−13]** specifically measured the LAP activity of human serum (Figure S8).

Compared with colorimetric assays, a fluorescence assay has many advantages. For instance, whereas fluorescence assays can be performed at submicromolar concentrations of the probes, colorimetric assays require millimolar levels. Another advantage

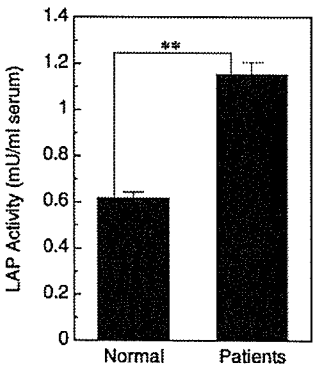

Figure 7. Difference of LAP activity in human sera between normal subjects and patients with cancer. Assay was performed in 10% serum with 1 μM **[Tb−13]**. Luminescence intensity (ex./em. = 330/545 nm) was measured for the initial 10 min using TRF measurement and converted to enzyme activity. In this case, 1 U was defined as the amount of protein which is required to hydrolyze 1 μmol of **[Tb−13]** per min at 37 °C, pH 7.4. Data are shown as mean ± SEM (n = 5). ** indicates a significant difference, $P < 0.01$.

is that simultaneous detection of different targets is possible using multiple fluorescent probes with different excitation or emission wavelengths. As one of the major disadvantages, i.e., background fluorescence, can be eliminated by means of TRF

measurements (see previous section), it is expected that TRF assays using lanthanide complexes such as **[Tb−13]** will be of great practical value.

Conclusions

We have designed and synthesized a series of lanthanide complexes, each consisting of three moieties: a lanthanide chelate, a luminescence off/on switch, and an antenna. As we had anticipated, quenching of lanthanide luminescence was observed as the HOMO energy level of the switch moiety became higher. By careful examination of the photochemical properties of these complexes, we demonstrated that the quenching of the complexes observed here is due to intramolecular PeT from the switch moiety to the antenna. This is the first report in which the effectiveness of intramolecular PeT as a mechanism for luminescence off/on switch has been studied. The luminescence off/on threshold for both Tb^{3+} and Eu^{3+} complexes was determined for the first time; this is critical information for the design of luminescence probes. These findings are an important step in establishing a rational method for the development of luminescence-based chemosensors.

By applying this novel approach of calculating the HOMO level of the switch moiety, we developed a luminescence probe for LAP, **[Ln−13]**. It was confirmed to be a sensitive probe for monitoring LAP activity on microplates, where the high background fluorescence could be eliminated by TRF measurement. **[Ln−13]** was also shown to be potentially useful in clinical diagnosis. It is noteworthy that the peptide sequence of **[Tb−13]** can be changed as desired, so that one can easily develop a luminescence probe for any desired protease.

The greatest advantage of our PeT-based approach is that the luminescence intensity of the complex can be predicted to a large extent by calculating the HOMO energy level of the switch moiety. The protease probe described here is not the only application of this approach. By selecting appropriate switch moieties, it can in principle be applied to every target species, including metal ions, enzymes, ROS, and so on.

Recently, a few groups have reported time-resolved luminescence imaging of lanthanide complexes.[46] For instance, we have developed a luminescence microscopy system which can obtain time-resolved images of cells, and we successfully visualized intracellular Zn^{2+} with virtually no background.[47] The development of rationally designed probes for molecules of interest, in combination with these imaging systems, will open a new frontier in fluorescence imaging.

Experimental Section

Materials. Boc-L-Leu-OH, HBTU, and HOBT·H_2O were obtained from Watanabe Chemical Industries, Ltd. (Japan). All other reagents for organic synthesis were purchased from Tokyo Kasei Co., Ltd. (Tokyo, Japan) or Wako Pure Chemical Industries, Ltd. (Osaka, Japan). Microsomal LAP (= aminopeptidase M) was purchased from Pierce Biochemistry, Inc. (Rockford, IL). Unless otherwise stated, 1 U is defined as the amount of protein which is required to hydrolyze 1 μmol of L-pNA per min at 25 °C, pH 7.2. Trypsin (from bovine pancreas), actinonin, amastatin hydrochloride, and bestatin hydrochloride were purchased from SIGMA (St. Louis, MO). Leu-pNA was purchased from Peptide Institute, Inc. (Osaka, Japan). Leu-MCA was purchased from Bachem AG (Bubendorf, Switzerland). Silica gel column chromatography was performed using silica gel 60N (Kanto Kagaku Co., Ltd., (Tokyo, Japan)). ODS column chromatography was performed using Chromatorex-ODS (Fuji Silysia Chemical Ltd., Japan).

Instruments. ^1H NMR and ^{13}C NMR spectra were recorded on a JEOL JNM-LA300. Mass spectra were recorded on a JEOL JMS-SX102A mass spectrometer (EI^+), a JEOL JMS-700 mass spectrometer (FAB^+), or a JEOL JMS-T100LC (ESI^+, ESI^-). Preparative HPLC purification was performed on a reversed-phase ODS column (GL Sciences (Tokyo, Japan), Inertsil Prep-ODS 30 mm × 250 mm) fitted on a JASCO PU-1587 HPLC system. UV−visible spectra were obtained on a Shimadzu UV-1600 (Tokyo, Japan). Fluorescence and phosphorescence spectroscopic studies were performed with a Hitachi F4500 (Tokyo, Japan). Time-resolved luminescence spectra and lanthanide luminescence lifetimes were obtained using a Perkin-Elmer LS-55 (Beaconsfield, Buckinghamshire, England). Luminescence assays on 96-well plates were performed using a plate reader instrument coupled with a Perkin-Elmer LS-55.

UV−visible Absorption Spectral Measurements. Absorption spectra of the complexes were measured at 5 μM in 100 mM HEPES buffer (pH 7.3, $I = 0.1$ ($NaNO_3$)). Each sample contained less than 0.1% DMSO as a cosolvent. Measurements were performed in 1 cm quartz cells at 25 °C.

Luminescence Spectral Measurements. Luminescence spectra of the complexes without a delay time were measured at 5 μM in 100 mM HEPES buffer (pH 7.3, $I = 0.1$ ($NaNO_3$)), following excitation at 330 nm. Each sample contained less than 0.1% DMSO as a cosolvent. Measurements were performed in 1 cm quartz cells at 25 °C. The excitation slit width was 2.5 nm (for Tb^{3+} complexes) or 5 nm (for Eu^{3+} complexes). The emission slit width was 2.5 nm. The photomultiplier voltage was 950 V.

Time-Delayed Luminescence Spectral Measurements. Time-delayed luminescence spectra of **[Ln−13]** (**Ln = Tb, Eu**) (5 μM) were measured in 100 mM HEPES buffer (pH 7.3, $I = 0.1$ ($NaNO_3$)), with a delay time of 50 μs and a gate time of 2.0 ms, after a 10 μs pulsed excitation at 330 nm. Each sample contained less than 0.1% DMSO as a cosolvent. Measurements were performed in 1 cm quartz cells at 25 °C. The excitation slit width was 2.5 nm (for Tb^{3+} complexes) or 5 nm (for Eu^{3+} complexes). The emission slit width was 2.5 nm.

Quantum Yield Measurements. Quantum yields of the complexes were estimated by a relative method with reference to a luminescence standard. For Tb^{3+} complexes, quinine sulfate ($\Phi = 0.546$ in 1 N H_2SO_4)[37] was used as a standard. For Eu^{3+}, $[Ru(bpy)_3]Cl_2$ ($\Phi = 0.028$ in air-equilibrated water)[38] was used. The quantum yields were calculated by eq 2,

$$\Phi_x/\Phi_{st} = [A_{st}/A_x][n_x^2/n_{st}^2][D_x/D_{st}] \quad (2)$$

where Φ is the quantum yield (subscript "st" stands for the reference, and "x", for the sample), A is the absorbance at the excitation wavelength, n is the refractive index (if both spectra are obtained in the aqueous solution, this term is canceled), and D is the area under the luminescence spectra on an energy scale. The sample and the reference were excited at the same wavelength (330 nm), where the absorbance was kept lower than 0.07. The luminescence spectra were measured at 25 °C in 100 mM HEPES buffer (pH 7.3, $I = 0.1$ ($NaNO_3$)) containing less than 0.1% DMSO as a cosolvent. All spectra were obtained with a Hitachi F4500 spectrofluorometer.

Estimation of the Lowest Triplet Energy Level. Lowest triplet energy levels (T_1) were calculated from the wavelength of the first peak of phosphorescence spectra. Phosphorescence spectra of **[Gd−X]** (**X = 1−12**) (20 μM) were measured at 77 K in MeOH/EtOH = 1:1, following excitation at 330 nm. Experiments were performed with

(46) (a) Faulkner, S.; Pope, S. J. A.; Burton-Pye, B. P. *Appl. Spectrosc. Rev.* **2005**, *40*, 1−31. (b) Weibel, N.; Charbonnière, L. J.; Guardigli, M.; Roda, A.; Ziessel, R. *J. Am. Chem. Soc.* **2004**, *126*, 4888−4896. (c) Charbonnière, L.; Ziessel, R.; Guardigli, M.; Roda, A.; Sabbatini, N.; Cesario, M. *J. Am. Chem. Soc.* **2001**, *123*, 2436−2437.
(47) Hanaoka, K.; Kikuchi, K.; Kobayashi, S.; Nagano, T. Manuscript in preparation.

a Hitachi F4500 equipped with a low-temperature phosphorescence measurement unit.

Luminescence Lifetime Measurements. Luminescence lifetimes were measured in both H_2O (100 mM HEPES buffer, pH 7.4) and D_2O (100 mM HEPES buffer, pD 7.4). The luminescence intensity (ex. 330 nm, em. 545 nm (Tb^{3+} complexes) or 615 nm (Eu^{3+} complexes)) at every 10 μs after pulsed excitation was measured using a 10 μs gate time. Data were fitted to a single-exponential decay curve (eq 3), where I and I_0 are the luminescence intensity at time t and time 0, respectively, and τ is the luminescence lifetime.

$$I = I_0 \exp(-t/\tau) \tag{3}$$

Enzymatic Reaction with LAP. All reactions were performed in a quartz cell at 37 °C. LAP (0.01 U) was dissolved in 100 mM Tris-HCl buffer (pH 7.4) and incubated for 5 min, before 2 μM **[Ln−13]** (**Ln = Tb, Eu**) was added. The reaction volume was 3.0 mL, and the solution contained less than 0.1% DMSO as a cosolvent. Luminescence spectra were measured at every 5 min after the addition of the probe without a delay time. Control experiments were performed by replacing LAP or **[Ln−13]** with other reagents.

Estimation of Inhibitory Activity. Various amounts of inhibitors were added to 100 mM Tris-HCl buffer (pH 7.4) along with LAP (0.01 U), and the mixtures were incubated for 5 min at 37 °C, followed by the addition of **[Tb−13]** (2 μM). The total reaction volume was 3.0 mL, and the solution contained less than 0.1% DMSO as a cosolvent. Luminescence intensity (ex. 330 nm, em. 545 nm) was measured continuously up to 5 min at 37 °C. The initial velocity of the reaction was calculated from the change of intensity during the first 3 min, where the luminescence decreased in a linear fashion. Inhibitory activity (%) was determined by comparing the velocity in the presence and absence of the inhibitor. Studies using Leu-MCA were performed with the same procedure except for the measured wavelength (ex. 380 nm, em. 440 nm). For Leu-pNA, probe concentration was 20 μM, and the absorbance at 405 nm was recorded. The inhibition constant (K_i) was calculated from the following equation (eq 4), where v = reaction velocity in the presence of inhibitor, v_0 = reaction velocity in the absence of inhibitor, and [I] = inhibitor concentration.

$$\frac{v}{v_0} = \frac{1}{1 + [\mathrm{I}]/K_i} \tag{4}$$

Determination of Kinetic Parameters. Various concentrations of the probes (= Leu-pNA, Leu-MCA, **[Tb−13]**) were dissolved in 100 mM Tris-HCl buffer (pH 7.4). LAP (0.001 U/ml, final concentration) was added to the solution, and the luminescence intensity (or absorbance) was recorded continuously as described above. The initial reaction velocity was calculated, plotted against probe concentration, and fitted to a Michaelis−Menten curve. K_m and k_{cat} were determined by the least-squares method.

Analytical HPLC. To confirm that enzymatic cleavage of the leucine moiety had taken place, analytical RP-HPLC was performed using an Inertsil 3 ODS column (4.6 mm × 250 mm, GL Sciences, Japan), fitted on a JASCO PU-980 HPLC system. Conditions: linear gradient from 15% to 45% solvent B (solvent A, 0.1 M triethylammonium acetate (pH 7.4); solvent B, 80% acetonitrile/20% 0.1 M triethylammonium acetate (pH 7.4)).

LAP Assay on 96-Well Plates. Experiments were performed on PLL-coated black plates (clear bottom) (Iwaki, Japan) at room temperature. First, LAP was added to 100 mM Tris-HCl buffer (pH 7.4). For wells with inhibitor, amastatin (10 μM) was added at the same time. After 10 min, **[Tb−13]** was added to the wells, the total volume of which was 0.2 mL. The plate was incubated for 60 to 90 min, and then the luminescence intensity (ex. 325 nm, em. 545 nm) was measured with delay and gate times of 50 μs and 2.0 ms, respectively. The excitation and emission slits were 10 nm. An assay using Leu-MCA was performed with the same procedure except for the measured wavelength (ex. 380 nm, em. 440 nm) and without a delay time.

Assay of Human Serum (Using Tb Complex). Human sera from 5 healthy volunteers (normal) and 5 patients with cancer of the hepato-biliary-pancreatic systems (patients) were diluted 10 times with Tris-HCl buffer (0.1 M, pH 7.4). Then 1 μM **[Tb−13]** was added to the solution, and a TRF measurement was performed as described above at 37 °C. Enzymatic activity was calculated from the change of luminescence over the first 10 min. 1 U was defined as the enzymatic activity that cleaved 1 μmol of **[Tb-13]** per min under the assay conditions.

Assay of Human Serum (Using a Commercially Performed Method). The following experiments were performed by SRL, Inc. (Tokyo, Japan). Briefly, the substrate l-leucyl-3,5-dibromo-4-hydroxyanilide (L-Leu-DBHA) was converted by LAP in the sample to 3,5-dibromo-4-hydroxyanilide, which was coupled to *N*-ethyl-*N*-(2-hydroxy-3-sulfopropyl)-*m*-toluidine (TOOS) by another enzyme, bilirubin oxidase (BOD), to yield a green pigment. The absorbance of the pigment at 700 nm was recorded by a Hitachi 7170 autoanalyzer as a measure of the LAP activity of the sample. Experiments were performed at 37 °C.

Supporting Information Available: Synthetic procedures of **[Ln−X]** (**Ln = Tb, Eu**) (**X = 1−13**); photophysical properties of the complexes; comparison of kinetic parameters; inhibition constants of LAP inhibitors; emission spectra of **[Eu−8]** and **[Eu−1]**; comparison of luminescence intensity before and after the enzymatic reaction; spectral change of **[Ln−13]** upon reaction with LAP; emission intensity of **[Ln−X]** after the addition of LAP or trypsin; HPLC chart of **[Ln−X]**; LAP reaction of **[Tb−13]** on 96-well plate; limit of detection of LAP using two probes; correlation between LAP activity measured by the two methods; serum LAP assay in the presence of amastatin; list of authors of ref 19b. This material is available free of charge via the Internet at http://pubs.acs.org.

JA060729T

Journal of Neuroscience Research 83:167–176 (2006)

Inhibition of Presynaptic Activity by Zinc Released From Mossy Fiber Terminals During Tetanic Stimulation

Akira Minami,[1] Naomi Sakurada,[1] Sayuri Fuke,[1] Kazuya Kikuchi,[2] Tetsuo Nagano,[2] Naoto Oku,[1] and Atsushi Takeda[1]*

[1]Department of Medical Biochemistry, School of Pharmaceutical Sciences, University of Shizuoka, Shizuoka, Japan
[2]Laboratory of Bioorganic and Medicinal Chemistry, Graduate School of Pharmaceutical Sciences, The University of Tokyo, Tokyo, Japan

Zinc exists in high densities in the giant boutons of hippocampal mossy fibers. On the basis of the evidence that zinc decreases extracellular glutamate concentration in the hippocampus, the presynaptic action of zinc released from mossy fibers during high-frequency (tetanic) stimulation was examined using hippocampal slices. The increase in zinc-specific fluorescent signals was observed in both extracellular and intracellular compartments in the mossy fiber terminals during the delivery of tetanic stimuli (100 Hz, 1 sec) to the dentate granule cell layer, suggesting that zinc released from mossy fibers is immediately retaken up by mossy fibers. When mossy fiber terminals were preferentially double-stained with zinc and calcium indicators and tetanic stimuli (100 Hz, 1 sec) were delivered to the dentate granule cell layer, the increase in calcium orange signal during the stimulation was enhanced in mossy fiber terminals by addition of CaEDTA, a membrane-impermeable zinc chelator, and was suppressed by addition of zinc. The decrease in FM4-64 signal (vesicular exocytosis) during tetanic stimulation (10 Hz, 180 sec), which induced mossy fiber long-term potentiation, was also enhanced in mossy fiber terminals by addition of CaEDTA and was suppressed by addition of zinc. The present study demonstrates that zinc released from mossy fibers may be a negative-feedback factor against presynaptic activity during tetanic stimulation.

Key words: mossy fiber zinc; neuromodulator; calcium; exocytosis; tetanic stimulation

The long-term potentiation (LTP) in hippocampal mossy fiber synapses is independent of N-methyl-D-aspartate (NMDA) receptor activation. The LTP is expressed by presynaptic mechanisms leading to persistent enhancement of neurotransmitter release. The induction of mossy fiber LTP is critically dependent on the rise in presynaptic calcium induced by high-frequency (tetanic) stimulation (Castillo et al., 1994; Nicoll and Malenka, 1995; Breustedt et al., 2003), which activates the calcium-calmodulin-sensitive adenyl cyclase I (Wang and Storm, 2003). This enzyme is abundant in mossy fiber terminals. Mossy fiber LTP is independent of the rise in postsynaptic calcium (Mellor and Nicoll, 2001). However, there is evidence that postsynaptic factors also participate in induction of mossy fiber LTP. For example, mossy fiber LTP is induced by postsynaptic photolysis of caged calcium compounds to elevate postsynaptic calcium level (Wang et al., 2004), whereas it is blocked by postsynaptic injection of ephrin-B receptor tyrosine kinase inhibitors (Contractor et al., 2002) or calcium chelators (Williams and Johnston, 1989; Yeckel et al., 2001; Alle et al., 2001). Thus, the role of the rise in postsynaptic calcium in mossy fiber LTP is controversial.

As a characteristic of mossy fibers, all giant boutons of mossy fibers contain zinc in the presynaptic vesicles (Danscher, 1981; Sindreu et al., 2003), and the zinc concentration is estimated to be approximately 300 μM (Frederickson et al., 1983). Zinc is released by tetanic stimulation (10–100 Hz; Li et al., 2001a; Ueno et al., 2002), which induces the mossy fiber LTP (Kobayashi et al., 1996). Zinc inhibits NMDA (Peters et al., 1987; Westbrook and Mayer, 1987; Paoletti et al., 1997; Traynelis et al., 1998) and γ-aminobutyric acid (GABA; Westbrook and Mayer, 1987; Smart et al., 1994) receptors, although it potentiates α-amino-3-hydroxy-5-methyl-4-isoxazolepropionate (AMPA)/kainate receptor (Rassendren et al., 1990). Glutamate (Vandenberg et al., 1998) and GABA (Cohen-Kfir et al., 2005) transporters and voltage-dependent calcium channels (VDCC; Busselberg et al., 1992) are inhibited by zinc. Lu et al. (2000) demonstrate that the acute depletion of bouton

*Correspondence to: Atsushi Takeda, Department of Medical Biochemistry, School of Pharmaceutical Sciences, University of Shizuoka, 52-1 Yada, Shizuoka 422-8526, Japan. E-mail: takedaa@u-shizuoka-ken.ac.jp

Received 18 September 2005; Revised 6 October 2005; Accepted 6 October 2005

Published online 7 December 2005 in Wiley InterScience (www.interscience.wiley.com). DOI: 10.1002/jnr.20714

zinc in the hippocampal slice with a membrane-permeable zinc chelator, dithizone, reversibly inhibits the induction of mossy fiber LTP, suggesting that endogeneous zinc is required for the induction of mossy fiber LTP. On the other hand, impairment of spatial learning, memory, or sensorimotor functions was not observed in zinc transporter-3-null mice, which lack the histochemically reactive zinc in synaptic vesicles (Cole et al., 2001). Furthermore, mossy fiber LTP is also induced in the presence of zinc chelators, 1,2-diethyl-3-hydroxypyridine-4-one (CP94) or CaEDTA (Xie and Smart, 1994; Vogt et al., 2000). Thus, the physiological significance of zinc as an endogenous neuromodulator is still poorly understood.

EDTA binds zinc with very high affinity, K_D $10^{-16.4}$, and the apparent affinity constant of CaEDTA for zinc is in the range of 3–4 nM (Dawson et al., 1986; Bers et al., 1994). CaEDTA (2.5 mM) has no appreciable effect at low stimulation frequencies as measured by extracellular field excitatory postsynaptic potential (fEPSP) mediated by AMPA-type glutamate receptors, and mossy fiber LTP is minimally influenced by chelating extracellular zinc with CaEDTA (Vogt et al., 2000). The effect of CaEDTA (1 mM) on the induction of mossy fiber LTP was also minimal in a study by Li et al. (2001b). By judging from the increased rates (around 10%) of fEPSP by CaEDTA in both cases, however, it is possible that zinc released from mossy fibers has an action in the induction of LTP. On the other hand, there is almost no report on zinc's action in the change of presynaptic activity during LTP induction (tetanic stimulation). This is potentially an important issue in understanding not only the mossy fiber LTP but also the role of mossy fiber zinc.

On the basis of the evidence that zinc decreases extracellular glutamate concentration in the hippocampus (Takeda et al., 2003, 2004), the present study examined the presynaptic action of zinc released from mossy fibers during tetanic stimulation by using hippocampal slices. The presynaptic activity was evaluated by intracellular calcium signal and vesicular exocytosis.

MATERIALS AND METHODS

Chemicals

Calcium orange AM, a membrane-permeable calcium indicator, and FM4-64, an indicator of presynaptic activity, were purchased from Molecular Probes (Eugene, OR) and Sigma (St. Louis, MO), respectively. ZnAF-2 and ZnAF-2 DA, a membrane-impermeable and a membrane-permeable zinc indicators, respectively, were kindly supplied by Daiichi Pure Chemicals Co., Ltd. (Tokyo, Japan). These fluorescent indicators were dissolved in dimethyl sulfoxide (DMSO) and then diluted in artificial cerebrospinal fluid (ACSF) containing 124 mM NaCl, 2.5 mM KCl, 1.0 mM $MgCl_2$, 1.25 mM NaH_2PO_4, 2.0 mM $CaCl_2$, 26 mM $NaHCO_3$, and 10 mM D-glucose (pH 7.3). To facilitate cellular uptake of membrane-permeable indicators, cremophore EL (Sigma) was added to DMSO solutions (final concentration 0.02%).

Hippocampal Slice Preparation

Wistar rats (4–5 weeks old, Japan SLC, Hamamatsu, Japan) were anesthetized with ether and decapitated in accordance with the Japanese Pharmacological Society guide for the care and use of laboratory animals. The brain was quickly removed and immersed in ice-cold choline-ACSF containing 124 mM choline chloride, 2.5 mM KCl, 2.5 mM $MgCl_2$, 1.25 mM NaH_2PO_4, 0.5 mM $CaCl_2$, 26 mM $NaHCO_3$, and 10 mM glucose (pH 7.3) to suppress excessive neuronal excitation. Horizontal hippocampal slices (400 μm) were prepared by using a vibratome ZERO-1 (Dosaka, Kyoto, Japan) in an ice-cold choline-ACSF. Slices were then maintained in ACSF at 25°C for at least 30 min. All solutions used in the experiments were continuously bubbled with 95% O_2 and 5% CO_2.

Hippocampal Mossy Fiber Imaging

For intracellular zinc imaging, the hippocampal slices were loaded with 10 μM ZnAF-2 DA for 30 min, then washed out with ACSF for at least 30 min. The hippocampal slices were transferred to a recording chamber filled with ACSF. For extracellular zinc imaging, the hippocampal slices were directly transferred to a recording chamber filled with 10 μM ZnAF-2. Fluorescence was imaged with an Argus-50/CA system (Hamamatsu Photonics, Hamamatsu, Japan) with a cooled CCD camera (excitation 490 nm, dichroic beam splitter 505 nm) at 25°C.

Electrical Stimulation and Imaging

For intracellular calcium and extracellular zinc imaging during electrical stimulation, the hippocampal slices were loaded with 10 μM Fura-2 AM for 30 min and then transferred a chamber filled with ACSF to wash out extracellular Fura-2 AM for at least 30 min. The hippocampal slices were transferred to a recording chamber filled with 10 μM ZnAF-2. In the case of intracellular zinc imaging, the hippocampal slices were loaded with 10 μM ZnAF-2 DA for 30 min, then transferred a chamber filled with ACSF to wash out extracellular ZnAF-2 DA for at least 30 min. The hippocampal slices were transferred to a recording chamber filled with ACSF.

Electrical stimuli (100 Hz, 1 sec, 100 μA, 200 μsec/pulse) were delivered to the dentate granular cell layer through a bipolar tungsten electrode. The fluorescence of fura-2 (excitation 351 nm, monitoring 505–530 nm) and ZnAF-2 (excitation 488 nm, monitoring 505–530 nm) was measured in the stratum lucidum by using a confocal laser scanning microscopic system LSM 510 (Carl Zeiss), equipped with an inverted microscope (Axiovert 200M; Carl Zeiss), at the rate of 1 Hz through a ×10 objective. The region of interest was set in the stratum lucidum based on ZnAF-2 signal, which is useful for determination of mossy fiber terminals.

In another experiment, mossy fiber terminals were preferentially imaged with zinc and calcium indicators according to previous papers (Regehr and Tank, 1991; Kamiya et al., 2002; see Fig 3a). The hippocampal slices were transferred to a chamber and regionally perfused at the rate of 1.6 ml/min with ACSF via a large delivery pipette and suction pipettes. A solution containing 10 μM ZnAF-2 DA and 10 μM calcium orange AM was regionally delivered to the stratum lucidum

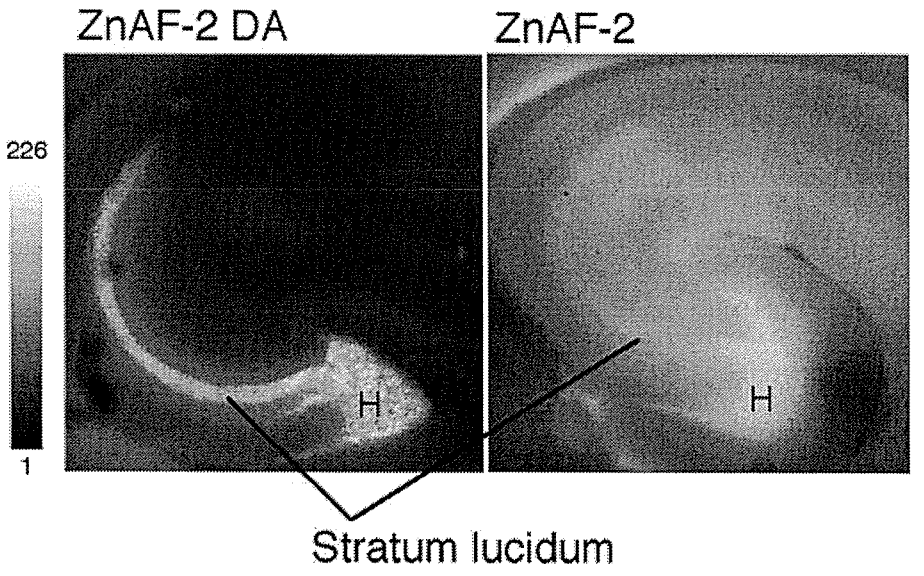

Fig. 1. Imaging of hippocampal intracellular and extracellular zinc. ZnAF-2 DA and ZnAF-2 were applied to rat hippocampal slices to image intracellular and extracellular zinc, respectively. The fluorescent signal was imaged with an Argus-50/CA system as described under Hippocampal mossy fiber imaging. H, hilus.

via a small delivery pipette at the rate of 15 μl/min for 30 min. Unloaded indicators were collected through a large suction pipette. The hippocampal slices were transferred to a recording chamber filled with ACSF or reagents in ACSF.

Electrical stimuli (100 Hz, 1 sec, 100 μA, 200 μsec/pulse) were delivered to the dentate granular cell layer through a bipolar tungsten electrode. The fluorescence of calcium orange (excitation 543 nm, monitoring above 560 nm) and ZnAF-2 (excitation 488 nm, monitoring 505–530 nm) was measured in the mossy fiber terminals with a confocal laser scanning microscopic system, LSM 510 META (Carl Zeiss), equipped with an inverted microscope (Axiovert 200M; Carl Zeiss), at the rate of 1 Hz through a ×20 objective.

Electrical Stimulation and Recordings

The mossy fiber-CA3 pyramidal neuron responses were induced by stimulation of the dentate granule cell layer with a bipolar tungsten electrode. Extracellular recordings were obtained by using glass micropipettes filled with 3 M NaCl (2–10 MΩ). The recording electrodes were placed along the trajectory of the mossy fiber pathway. To induce mossy fiber LTP, test stimuli were delivered to the dentate granule cell every 10 sec (0.1 Hz). The stimulus intensity was set to produce approximately 40% (100 μA, 200 μsec/pulse) of the maximal EPSP. Tetanic stimulation consisted of one train of 10 Hz lasting for 180 sec. The maximal amplitude of the mossy fiber-CA3 EPSP was calculated and normalized to the 30-min basal value (defined as 100%). At the beginning of the experiments for the LTP induction, the physiological state of the slices was tested by verifying the existence of paired-pulse facilitation, which was induced by application of paired pulses separated by 40 msec. Because of the complex circuitry of the CA3, the metabotropic glutamate receptor II agonist 2-(2,3-dicarboxy-cyclopropyl)glycine (DCG-IV) was used at the end of the experiments to verify that the signal was generated by mossy fiber inputs (Kamiya et al., 1996).

Mossy Fiber Terminal Activity

The hippocampal slices were transferred to an incubation chamber filled with ACSF containing 10 μM ZnAF-2DA, allowed to stand at 25°C for 30 min, transferred a chamber filled with ACSF to wash out extracellular ZnAF-2DA for at least 30 min, transferred to an incubation chamber filled with ACSF containing 5 μM FM4-64 and 45 mM KCl, allowed to stand at 25°C for 90 sec, transferred a chamber filled with ACSF to wash out extracellular FM4-64, and transferred to a recording chamber filled with ACSF or reagents in ACSF, in which 10 μM 6-cyano-7-nitroquinoxaline-2,3-dione (CNQX), an antagonist of AMPA/kainate receptors, was contained, to prevent recurrent activity. To chelate intracellular zinc, in another experiment the hippocampal slices were loaded with 50 μM 1-hydroxypyridine-2-thione (pyrithione; Molecular Probes), a membrane-permeable zinc chelator, for 90 sec. The hippocampal slices were transferred a chamber filled with ACSF to wash out extracellular pyrithione for at least 3 min and transferred to a recording chamber filled with ACSF containing 10 μM CNQX.

Electrical stimuli (10 Hz, 180 sec, 100 μA, 200 μsec/pulse) were delivered to the dentate granular cell layer through a bipolar tungsten electrode. The fluorescence of FM4-64 (excitation 488 nm, monitoring above 650 nm) and ZnAF-2 (excitation 488 nm, monitoring 505–530 nm) was measured with a confocal laser scanning microscopic system LSM 510 META at the rate of 1 Hz through a ×20 objective to observe attenuation of FM4-64 fluorescence (destaining) based on presynaptic activity. At the end of the experiments, complete depolarization-induced destaining was evoked by single strong stimuli (100 Hz, 18 sec, 100 μA, 200 μsec/pulse). The activity-dependent component of FM4-64 fluorescence in the mossy fiber terminals was measured for each punctum by subtracting its residual fluorescence intensity (<10% of initial intensity) measured after the strong electrical stimulation that produced maximal destaining. FM4-64 signal